JOURNAL OF GEOPHYSICAL RESEARCH, VOL. 105, NO. B3, PAGES 5695–5719, MARCH 10, 2000

Global Positioning System constraints on plate kinematics and dynamics in the eastern Mediterranean and Caucasus

S. McClusky,[1] S. Balassanian,[2] A. Barka,[3] C. Demir,[4] S. Ergintav,[5] I. Georgiev,[6] O. Gurkan,[7] M. Hamburger,[8] K. Hurst,[9] H. Kahle,[10] K. Kastens,[11] G. Kekelidze,[12] R. King,[1] V. Kotzev,[6] O. Lenk,[4] S. Mahmoud,[13] A. Mishin,[14] M. Nadariya,[12] A. Ouzounis,[15] D. Paradissis,[15] Y. Peter,[10] M. Prilepin,[14] R. Reilinger,[1] I. Sanli,[4] H. Seeger,[16] A. Tealeb,[13] M. N. Toksöz,[1] and G. Veis[15]

Abstract. We present and interpret Global Positioning System (GPS) measurements of crustal motions for the period 1988–1997 at 189 sites extending east-west from the Caucasus mountains to the Adriatic Sea and north-south from the southern edge of the Eurasian plate to the northern edge of the African plate. Sites on the northern Arabian platform move 18 ± 2 mm/yr at N25°± 5°W relative to Eurasia, less than the NUVEL-1A circuit closure rate (25 ± 1 mm/yr at N21°± 7°W). Preliminary motion estimates (1994–1997) for stations located in Egypt on the northeastern part of Africa show northward motion at 5–6 ± 2 mm/yr, also slower than NUVEL-1A estimates (10 ± 1 mm/yr at N2°± 4°E). Eastern Turkey is characterized by distributed deformation, while central Turkey is characterized by coherent plate motion (internal deformation of <2 mm/yr) involving westward displacement and counterclockwise rotation of the Anatolian plate. The Anatolian plate is de-coupled from Eurasia along the right-lateral, strike-slip North Anatolian fault (NAF). We derive a best fitting Euler vector for Anatolia-Eurasia motion of 30.7°± 0.8°N, 32.6°± 0.4°E, 1.2°± 0.1°/Myr. The Euler vector gives an upper bound for NAF slip rate of 24 ± 1 mm/yr. We determine a preliminary GPS Arabia-Anatolia Euler vector of 32.9°± 1.2°N, 40.3°± 1.1°E, 0.8°± 0.2°/Myr and an upper bound on left-lateral slip on the East Anatolian fault (EAF) of 9 ± 1 mm/yr. The central and southern Aegean is characterized by coherent motion (internal deformation of <2 mm/yr) toward the SW at 30 ± 1 mm/yr relative to Eurasia. Stations in the SE Aegean deviate significantly from the overall motion of the southern Aegean, showing increasing velocities toward the trench and reaching 10 ± 1 mm/yr relative to the southern Aegean as a whole.

1. Introduction

Earth scientists recognized early in the development of plate tectonics that plate boundaries in continental areas are substantially wider than those in oceanic

[1]Department of Earth, Atmospheric, and Planetary Sciences, Massachusetts Institute of Technology, Cambridge.

[2]National Survey for Seismic Protection, Yerevan, Armenia.

[3]Eurasian Earth Sciences Institute, Istanbul Technical University, Istanbul, Turkey.

[4]General Command of Mapping, Ankara, Turkey.

[5]Türkiye Bilimsel ve Teknik Arastirma Kurumu, Marmara Research Center, Gebze, Turkey.

Paper number 1999JB900351.
0148-0227/00/1999JB900351$09.00

[6]National Academy of Sciences, Geodesy Department, Sofia, Bulgaria.

[7]Kandilli Observatory, Bogazici Univ., Istanbul, Turkey.

[8]Department of Geological Sciences, Indiana University, Bloomington.

[9]Jet Propulsion Laboratory, Pasadena, California.

[10]Institut fur Geodasie und Photogrammetrie, ETH Honggerberg, Zurich, Switzerland.

[11]Lamont-Doherty Earth Observatory of Columbia University, Palisades, New York.

[12]Department of Geodesy and Cartography of Georgia, Tbilisi, Georgia.

[13]National Research Institute of Astronomy and Geophysics, Helwan, Egypt.

[14]Joint Institute of Physics of the Earth, Moscow, Russia.

[15]Higher Geodesy Laboratory, National Technical University, Athens, Greece.

[16]Bundesamt fur Kartographie und Geodasie, Frankfurt, Germany.

plates [*Isacks et al.,* 1968; *McKenzie,* 1970; *Molnar and Tapponier,* 1975]. The underlying causes for this different behavior as well as the most appropriate way of describing continental deformation (i.e., continuum deformation versus microplate or block behavior) remain the subject of ongoing debate [e.g., *Avouac and Tapponier,* 1993; *Houseman and England,* 1993; *Thatcher,* 1995]. The Global Positioning System (GPS) is providing an important new tool to quantify continental deformation to a precision and on a scale unprecedented in the Earth sciences [e.g., *Dixon,* 1991; *Hager et al.,* 1991]. These new constraints on the kinematics of continental deformation are, in turn, providing constraints on rheological models of the continental lithosphere and the forces responsible for active deformation [e.g., *Thatcher,* 1995]. In this paper we integrate GPS observations collected over the past 9 years (1988–1997) for a large part of the eastern Mediterranean region in the zone of interaction of the Arabian, African, and Eurasian plates and consider the implications for the nature of contemporary tectonic processes in this plate collision zone. The present paper extends the work of *Reilinger et al.* [1997a] by including GPS results for the Aegean and North Africa as well as new data from 1996 and 1997 surveys in Turkey and the Caucasus, which more tightly constrain velocity estimates and provide denser spatial coverage throughout this region.

Plate 1 is a schematic tectonic map of the eastern Mediterranean/Middle East region. This region has been identified as an ideal natural laboratory for studying the kinematics and dynamics of plate interactions [e.g., *Plag et al.,* 1998] because of the wide variety of tectonic processes encompassed, including various stages of continental collision (Zagros/Caucasus/Black Sea), subduction of oceanic lithosphere and associated back arc spreading (Cyprus/Hellenic/Calabrian arcs, Aegean and Tyrrhenian Seas), continental extension (western Turkey/Marmara Sea/Gulf of Corinth), continental "escape" (Anatolia), major continental strike-slip faults (North and East Anatolian and Dead Sea faults), and a variety of smaller-scale processes associated with African-Arabian-Eurasian plate interactions. All of these processes are contained within an area with linear dimensions of roughly 2000 km. Furthermore, the eastern Mediterranean region has a remarkably long historic record of major earthquakes [e.g., *Ambraseys,* 1975; *Ambraseys and Jackson,* 1998] and has been the focus of intense geologic and geophysical investigations [e.g., *Sengor et al.,* 1985; *Spakiman,* 1991; *Mueller and Kahle,* 1993; *De Jonge et al.,* 1994].

The tectonic framework of the eastern Mediterranean is dominated by the collision of the Arabian and African plates with Eurasia [*McKenzie,* 1970; *Jackson and McKenzie,* 1984, 1988]. Plate tectonic models [*DeMets et al.,* 1990; *Jestin et al.,* 1994] based on analysis of global seafloor spreading, fault systems, and earthquake slip vectors indicate that the Arabian plate is moving in a north-northwest direction relative to Eurasia at a rate of about 18–25 mm/yr, averaged over about 3 Myr. These models also indicate that the African plate is moving in a northerly direction relative to Eurasia at a rate of about 10 mm/yr (at 30°N, 31°E). Differential motion between Africa and Arabia (~10–15 mm/yr) is thought to be taken up predominantly by left-lateral motion along the Dead Sea transform fault. This northward motion results in continental collision along the Bitlis-Zagros fold and thrust belt, intense earthquake activity (Figure 1) and high topography in eastern Turkey and the Caucasus mountains (Plate 1), and westward extrusion of the Anatolian plate [*McKenzie,* 1970] (Anatolia is here defined as the region of Turkey west of the Karliova triple junction and lying between the East Anatolian and North Anatolian faults; Plate 1). The leading edge of the African plate is being subducted along the Hellenic arc at a higher rate than the relative northward motion of the African plate itself, requiring that the arc moves southward relative to Eurasia proper [e.g., *Sonder and England,* 1989; *Royden,* 1993]. Subduction of the African plate is also thought to occur along the Cyprean arc and/or the Florence rise south of Turkey, although it is less well defined in these regions than along the Hellenic arc.

A significant improvement to the simple three-plate model for the eastern Mediterranean region resulted from analysis of seismic information, field studies of surface faulting, and air/satellite images. Using such data, *McKenzie* [1970], *Jackson and McKenzie* [1988], and *Jackson* [1992] developed a plate tectonic framework for understanding deformation in the eastern Mediterranean and examined the principles that control continental tectonics in the region. They suggest that continental lithosphere tends to move laterally away from zones of compression, presumably to minimize topographic relief and to avoid subduction of buoyant continental material. They further suggest that the Anatolian plate moves westward from the zone of intense convergence in eastern Turkey, and they derive an Euler vector (i.e., rotation pole and rate) for Anatolia-Eurasia based on earthquake slip vectors along the North Anatolian fault (NAF) [*Jackson and McKenzie,* 1984]. Furthermore, they propose the existence of an Aegean plate that moves with a distinctly different velocity than the Anatolian plate and the separation of the two plates by a zone of north-south extension in western Turkey. This qualitative description, which has proven remarkably robust, is clearly illustrated by the distribution of earthquake focal mechanisms shown in Figure 1, which define the "aseismic" areas of Anatolia and the southern Aegean, a zone of N-S extension in western Turkey, and the major strike-slip faults which accommodate extrusion of Anatolia.

Space geodetic observations were initiated in the eastern Mediterranean region in the early 1980s and have helped to quantify broad-scale plate motions and the detailed deformations associated with plate interactions [e.g., *Wilson,* 1987; *Smith et al.,* 1994; *Straub and*

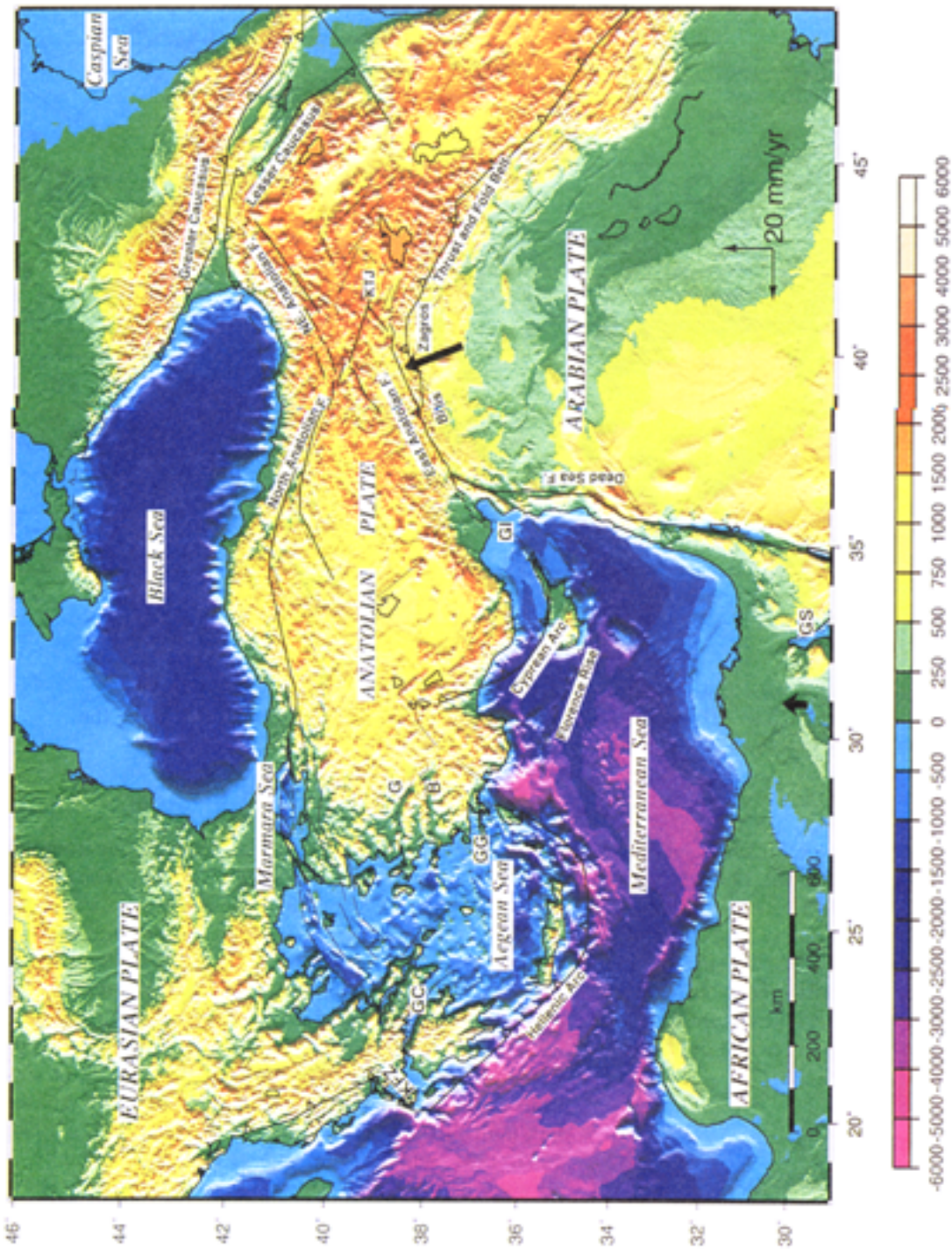

Plate 1. Simplified tectonic map of the eastern Mediterranean region superimposed on topography and bathymetry. Solid lines are strike-slip faults, lines with tick marks are normal faults with ticks on the downthrown block, and lines with triangles are thrust faults with triangles on the overriding block. Heavy arrows show NUVEL-1A plate motions relative to Eurasia. G, Gediz graben; B, Buyuk Menderes graben; KTJ, Karliova triple junction; GG, Gulf of Gokova; KFZ, Kephalonia fault zone; GI, Gulf of Iskenderun; GC, Gulf of Corinth; GS, Gulf of Suez.

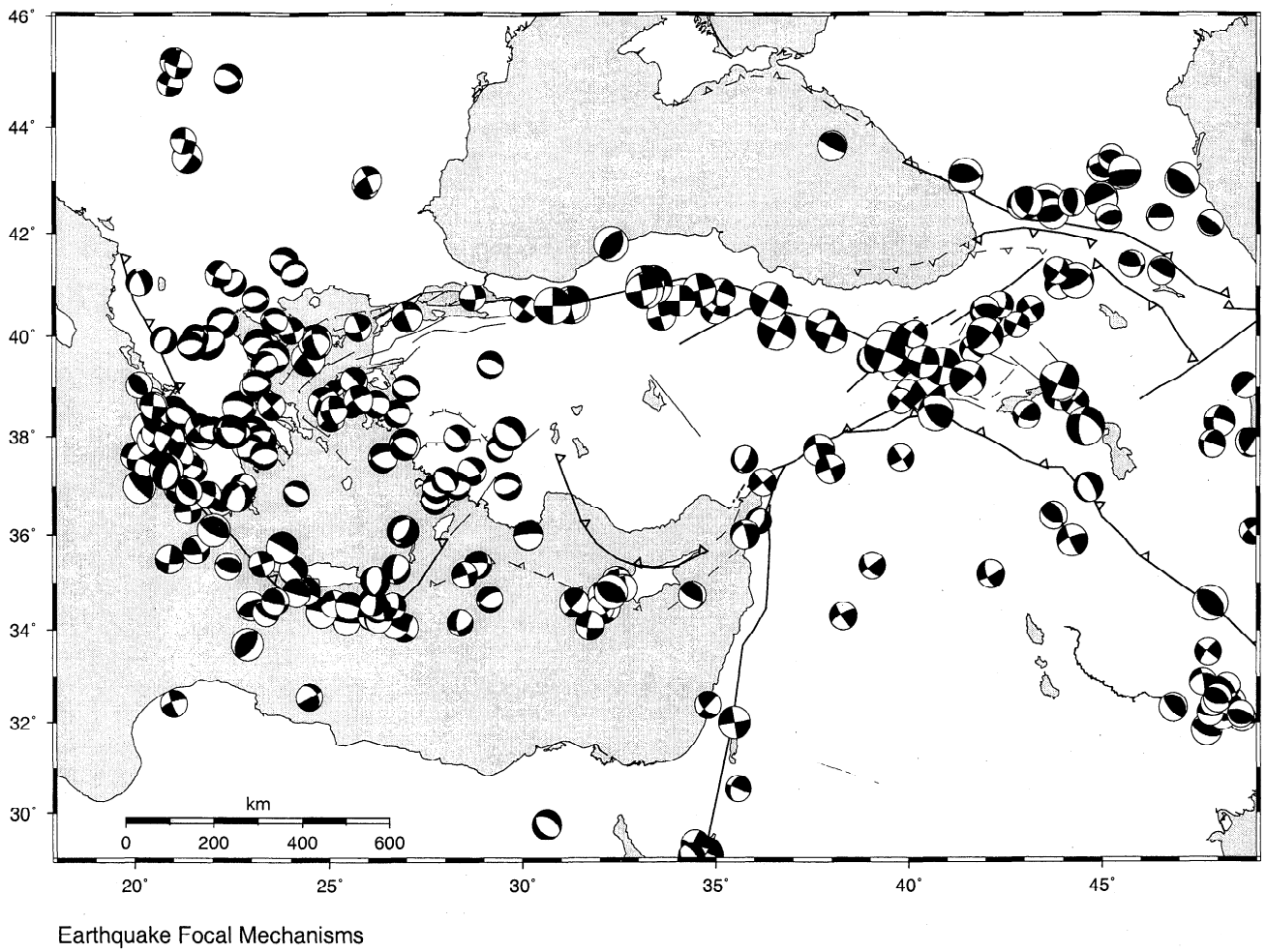

Figure 1. Focal mechanisms (lower hemisphere projection) for shallow (depth of <100 km), major earthquakes ($M > 5.0$) [*Dziewonski et al.*, 1981; *Jackson and McKenzie*, 1988] in the eastern Mediterranean region. Tectonic symbols are as in Plate 1.

Kahle, 1995; *Kahle et al.*, 1995; *Le Pichon et al.*, 1995; *Noomen et al.*, 1996; *Reilinger et al.*, 1997a,b; *Davies et al.*, 1997; *Plag et al.*, 1998]. In this study we present a comprehensive GPS-derived velocity field integrating data from the Caucasus, Turkey, North Africa, Israel, the Aegean, and Greece, including new observations made in 1996 and 1997, and consider the implications of observed motions for the kinematics and dynamics of plate interactions.

2. GPS Velocity Field

We initiated GPS measurements in the eastern Mediterranean region in 1988 and expanded and reobserved selected parts of the network each year between 1989 and 1997 except for 1995. The Aegean region of Greece was observed in 1988 (south), 1989 (north), 1992 (all), and 1996 (all) [*Gilbert et al.*, 1994]. In the West Hellenic Arc region of Greece, observations were made in 1989 (all), 1990, 1991 (all), 1992, 1993 (all), 1994, and 1996 [*Kahle et al.*, 1996]. The 1996 West Hellenic Arc survey mainly included observations from stations from the new Continuous Ionian Network (CION) [*Peter et al.*, 1998]. Between 1988 and 1992, measurements were concentrated during alternate years in western and eastern Turkey, with sufficient overlap to allow integration of the networks, but since the 1994 survey, almost all of the stations were reoccupied during each survey [*Reilinger et al.*, 1997a]. In addition to these broad-scale surveys in Turkey a small and relatively dense network of stations spanning the various strands of the North Anatolian fault in the Marmara region was observed in 1990, 1992, 1994, and 1996 [*Straub et al.*, 1997]. Finally, a network in the Caucasus was observed in 1991, 1994, and 1996 [*Reilinger et al.*, 1997b]. Table 1 gives a summary of the observations included in the current analysis. The earliest surveys in Turkey (1988–1990) and the West Hellenic Arc (1989–1992) were omitted. To aid in orbit determination and to strengthen the reference frame, in our analysis we also included data from 50 to 200 globally distributed stations from the International GPS Service (IGS) [*Beutler et al.*, 1993] acquired be-

Table 1. GPS Site Velocities and 1σ Uncertainties

Site	Lat	Lon	No.[a]	Span[b]	N Vel	Nσ[c]	E Vel	Eσ[c]	ρ_{EN}[d]
				Eastern Mediterranean Sites					
GORI	39.51	46.37	2	1994.8-1996.8	9.6	1.5	3.3	1.7	−0.05
JERM	39.84	45.66	2	1994.8-1996.8	10.1	1.4	4.6	1.5	−0.03
IJEV	40.91	45.14	2	1994.8-1996.8	7.4	1.4	4.0	1.4	−0.02
GARN	40.15	44.74	3	1991.6-1996.8	9.1	1.1	2.5	1.2	−0.01
NICH	41.83	44.53	3	1991.6-1996.8	5.8	1.2	1.1	1.2	0.00
NSSP	40.23	44.50	c	1996.8-1999.4	8.1	1.7	3.6	1.8	0.00
KRES	42.45	44.49	2	1994.8-1996.8	2.8	1.4	1.3	1.4	−0.01
MMOR	40.18	44.11	2	1994.8-1996.8	7.0	1.4	2.5	1.4	−0.01
ARTI	40.61	43.95	2	1994.8-1996.8	7.2	1.4	2.2	1.4	−0.02
NINO	41.54	43.89	2	1994.8-1996.8	4.2	1.4	0.9	1.4	−0.02
MATS	42.98	43.75	2	1994.8-1996.8	0.3	1.4	1.5	1.4	−0.03
LESO	42.49	43.54	3	1991.6-1996.8	−1.0	1.1	0.7	1.2	0.01
SFRE	42.49	43.40	3	1991.6-1996.8	1.9	1.2	−1.0	1.3	0.02
SACH	42.35	43.40	3	1991.6-1996.8	4.8	1.1	2.6	1.2	0.00
KHUR	42.58	43.38	3	1991.6-1996.8	−2.0	1.2	0.4	1.2	0.01
BALK	43.06	43.35	2	1996.8-1997.7	−0.4	2.4	−2.0	2.3	−0.10
KAL2	38.55	43.34	2	1994.8-1996.8	12.0	1.4	−5.3	1.5	0.00
KARS	40.69	43.17	3	1991.7-1996.8	5.2	1.1	0.7	1.2	0.00
KHOT	42.47	43.13	3	1991.6-1996.8	3.2	1.2	1.7	1.6	−0.05
ARGI	39.72	43.03	2	1994.8-1996.8	6.7	1.4	1.2	1.5	−0.02
PATN	39.24	42.91	3	1991.7-1996.8	8.7	1.1	−2.5	1.2	−0.02
BEUG	44.01	42.79	2	1994.8-1996.8	1.0	1.4	−0.6	1.4	−0.01
SHAT	43.74	42.67	3	1994.8-1997.7	1.7	1.3	0.3	1.4	−0.01
VANI	42.02	42.47	3	1991.6-1996.8	4.1	1.1	1.6	1.2	−0.02
SOLO	44.89	42.26	3	1994.8-1997.7	3.0	1.4	−2.6	1.4	−0.02
ULKA	43.35	42.19	2	1994.8-1996.8	−1.2	1.4	−0.9	1.5	−0.02
INGU	42.72	42.06	2	1994.7-1996.8	2.7	1.4	0.9	1.4	−0.02
OLTU	40.55	41.99	2	1994.7-1996.8	4.3	1.4	2.3	1.5	0.00
KRKT	38.75	41.79	2	1991.7-1994.8	14.4	1.2	−5.1	1.4	0.05
ZELB	43.79	41.56	4	1991.6-1997.7	0.8	1.0	0.5	1.1	−0.01
ZECK	43.79	41.56	c	1997.8-1999.4	0.8	1.0	0.5	1.1	−0.01
HOPA	41.37	41.34	2	1994.7-1996.8	2.6	1.4	−0.1	1.5	−0.01
ERZU	39.97	41.30	4	1991.7-1996.8	5.0	1.1	−0.9	1.2	−0.01
ISPI	40.44	40.81	3	1991.7-1996.8	2.5	1.1	0.2	1.2	−0.01
KIZI	37.25	40.65	2	1991.7-1997.8	16.1	1.2	−6.9	1.3	−0.02
MERC	39.73	40.25	3	1992.7-1996.8	4.9	1.2	−2.7	1.3	−0.02
KRCD	37.85	39.81	3	1992.7-1996.8	13.9	1.4	−7.6	1.5	−0.02
AKTO	40.97	39.70	4	1991.7-1996.8	1.7	1.1	0.5	1.2	0.00
KMAH	39.61	39.16	3	1992.7-1996.8	9.1	1.4	−19.6	1.4	−0.02
ADYI	37.75	38.23	2	1994.7-1996.8	13.4	1.4	−7.6	1.5	−0.02
MLTY	38.46	38.22	3	1991.7-1996.8	10.9	1.3	−12.0	1.3	−0.02
SINC	39.45	37.96	2	1991.7-1996.8	9.9	1.1	−18.3	1.2	−0.01
GAZI	36.90	37.57	3	1991.7-1996.8	12.3	1.1	−8.5	1.2	−0.02
MARS	37.52	37.00	2	1994.7-1996.8	8.8	1.4	−9.4	1.5	−0.01
SAKZ	37.19	36.97	2	1994.7-1996.8	10.3	1.4	−9.8	1.5	−0.01
SAMS	41.30	36.34	2	1994.7-1996.8	2.2	1.4	−0.1	1.5	0.01
DORT	36.90	36.14	2	1994.7-1996.8	8.6	1.4	−11.1	1.5	−0.02
SENK	36.05	36.13	2	1994.7-1996.8	7.9	1.4	−5.4	1.5	−0.01
KDRL	37.39	36.07	2	1991.7-1994.8	11.8	1.8	−12.2	2.2	0.18
ULUC	36.46	35.94	2	1991.7-1994.8	9.0	1.6	−11.5	1.7	−0.01
KATZ	32.99	35.69	c	1997.8-1999.4	11.2	2.2	−2.2	2.3	−0.01
SINO	42.02	35.21	3	1992.7-1996.8	0.8	1.2	−1.1	1.3	0.00
BARG	31.72	35.09	2	1994.7-1996.8	6.0	1.9	−0.2	2.0	−0.02
KKIR	40.45	34.88	2	1994.7-1996.8	4.8	1.4	−16.6	1.5	−0.02
YOZG	39.80	34.81	4	1991.7-1996.8	4.4	1.2	−21.0	1.3	−0.02
ABDI	39.11	34.80	2	1994.7-1996.8	2.2	1.9	−18.8	2.0	−0.02
TELA	32.07	34.78	2	1996.8-1998.2	8.6	1.7	−2.3	1.8	−0.02
MERS	36.90	34.55	2	1994.7-1996.8	3.8	1.4	−13.1	1.5	−0.01
NICO	35.14	33.40	c	1997.8-1999.4	4.1	2.4	−5.3	2.7	0.00
MELE	37.38	33.19	4	1991.7-1996.8	2.2	1.1	−14.1	1.1	−0.03
ANKR	39.89	32.76	c	1995.5-1999.4	−2.2	0.9	−20.8	1.0	−0.04
ANKA	39.87	32.73	3	1991.7-1996.8	−2.2	0.9	−20.8	1.0	−0.04

Table 1. (continued)

Site	Lat	Lon	No.[a]	Span[b]	N Vel	Nσ[c]	E Vel	Eσ[c]	ρ_{EN}[d]
				Eastern Mediterranean Sites (continued)					
ISME	40.88	32.57	3	1992.7-1996.8	−0.5	1.2	−8.1	1.2	−0.01
HALI	41.52	32.23	2	1994.7-1996.8	−1.1	1.4	0.8	1.4	−0.03
SEKI	36.43	32.16	2	1994.7-1996.8	0.5	1.4	−10.0	1.5	−0.03
SIVR	39.56	31.81	2	1992.7-1994.8	−3.1	1.2	−20.6	1.4	0.00
YIG2	40.94	31.44	2	1992.7-1994.8	−0.7	1.0	−3.9	1.0	−0.03
HELW	29.86	31.34	3	1994.7-1997.8	5.7	1.4	−2.1	1.6	−0.04
MEST	29.51	30.89	2	1994.7-1997.8	5.1	1.4	−2.0	1.6	−0.04
PINA	40.56	30.86	3	1990.7-1994.8	−1.4	2.1	−15.9	2.2	0.08
KDER	40.74	30.83	4	1990.7-1996.7	−1.2	1.5	−7.2	1.5	0.02
TEBA	40.39	30.80	4	1990.7-1996.7	−3.2	1.2	−19.9	1.2	0.01
AGOK	40.59	30.76	2	1994.7-1996.8	−2.1	1.3	−13.1	1.3	−0.02
KMAL	40.65	30.75	3	1990.7-1994.8	0.8	2.2	−9.9	2.2	0.14
AGUZ	40.54	30.68	2	1994.7-1996.8	−1.3	1.5	−17.2	1.4	−0.02
BOZT	40.55	30.68	3	1990.7-1994.8	−1.7	2.3	−15.9	2.2	0.10
KKAP	40.63	30.66	3	1990.7-1994.8	−3.2	1.9	−13.0	2.0	0.07
AFYO	38.77	30.64	3	1992.7-1996.8	−3.2	1.2	−21.6	1.2	−0.03
KTOP	40.61	30.64	3	1990.7-1994.8	−1.2	1.2	−13.2	1.2	−0.01
ESKI	39.66	30.64	3	1992.7-1996.8	−2.6	1.4	−24.4	1.5	−0.01
ANTG	36.83	30.61	2	1994.7-1996.8	−8.7	1.4	−10.1	1.4	−0.03
BURD	37.69	30.30	3	1992.7-1996.8	−8.4	1.2	−19.5	1.2	−0.04
SMAS	40.69	30.13	2	1994.7-1996.8	−0.9	1.3	−13.3	1.4	−0.02
SISL	40.74	30.13	2	1994.7-1996.8	−2.3	1.5	−8.2	1.5	−0.02
MEKE	40.47	30.03	3	1992.7-1996.8	−1.3	1.1	−17.1	1.2	−0.03
IUCK	40.42	29.93	2	1994.7-1996.8	−2.4	1.3	−18.6	1.3	−0.02
IGAZ	40.44	29.91	2	1994.7-1996.8	−2.6	1.5	−17.9	1.4	−0.02
DERB	40.36	29.68	3	1990.7-1994.8	1.0	2.0	−19.2	2.2	0.09
KASO	36.19	29.65	3	1992.7-1996.8	−10.2	1.2	−11.1	1.4	−0.03
YUHE	40.80	29.64	3	1990.7-1994.8	0.6	2.0	−5.7	2.2	0.09
OLUK	40.67	29.58	3	1990.7-1994.8	1.0	2.0	−13.1	2.1	0.09
IIMZA	40.16	29.51	3	1990.7-1994.8	−1.5	2.1	−21.5	2.2	0.10
SIRA	36.72	29.44	2	1994.7-1996.8	−10.8	1.4	−13.4	1.5	−0.02
CATA	40.20	29.26	3	1990.7-1994.8	−2.8	1.9	−21.5	2.0	0.10
GEML	40.46	29.15	3	1990.7-1994.8	1.1	2.0	−20.0	2.0	0.10
CINA	40.64	29.14	2	1992.7-1994.8	0.0	1.4	−15.9	1.4	−0.03
ULDA	40.12	29.14	4	1991.7-1996.8	−1.5	1.2	−20.1	1.3	−0.03
PAMU	37.94	29.14	2	1992.7-1994.8	−8.1	1.1	−21.5	1.2	−0.04
ZEYA	40.17	29.11	3	1990.7-1994.8	−1.9	1.9	−21.0	2.0	0.09
DTAS	40.27	29.11	3	1990.7-1994.8	−1.0	1.9	−21.2	2.0	0.09
ULUD	40.14	29.10	4	1990.7-1996.7	−4.3	1.3	−23.5	1.4	0.00
IKAN	41.06	29.06	5	1992.7-1996.8	−0.1	1.1	−2.5	1.1	−0.03
YIGE	40.17	29.02	3	1990.7-1994.8	−1.0	1.9	−22.6	2.0	0.09
ITAY	41.10	29.02	5	1990.7-1996.7	−0.1	1.2	−1.5	1.3	−0.03
GIRE	39.93	28.92	3	1990.7-1994.8	−2.1	2.0	−24.2	2.1	0.07
HAGA	40.17	28.78	3	1990.7-1994.8	−3.8	1.9	−20.3	2.0	0.09
DMIR	39.05	28.67	2	1992.7-1996.8	−6.8	1.1	−20.9	1.2	−0.04
ALSE	38.31	28.48	3	1992.7-1996.8	−12.6	1.4	−22.7	1.5	−0.02
MULA	37.17	28.43	1	1996.8-1996.8	−21.3	2.0	−16.9	2.0	−0.01
YENI	40.40	28.37	1	1996.8-1996.8	−3.9	2.0	−21.4	2.1	0.01
CINE	37.61	28.08	3	1992.7-1996.8	−20.2	1.2	−19.3	1.2	−0.04
ODME	38.25	28.00	3	1992.7-1996.8	−13.5	1.4	−21.0	1.4	−0.03
MARM	36.77	27.96	3	1992.7-1996.8	−25.5	1.2	−13.6	1.2	−0.04
MAER	40.97	27.96	3	1992.7-1996.7	−1.5	1.3	2.5	1.3	−0.02
BALI	39.72	27.91	3	1992.7-1996.8	−5.3	1.2	−22.3	1.3	−0.03
AKGA	39.01	27.87	2	1992.7-1994.8	−10.9	1.2	−20.3	1.2	−0.03
CAMK	37.20	27.84	2	1994.7-1996.8	−25.6	1.4	−16.0	1.4	−0.02
ERDE	40.40	27.82	7	1990.7-1996.8	−2.5	1.2	−19.1	1.3	0.00
KATV	35.95	27.78	4	1988.8-1996.8	−28.9	1.2	−8.0	1.3	0.03
DEMI	41.83	27.78	3	1992.7-1996.8	−1.2	1.2	0.6	1.2	−0.03
KOCB	40.06	27.76	3	1990.7-1994.8	−3.7	1.9	−23.7	1.9	0.06
UKIR	40.24	27.63	3	1990.7-1994.8	−5.0	2.0	−18.2	1.9	0.10
D7DU	39.29	27.59	2	1992.7-1994.8	−11.6	2.6	−15.9	2.5	−0.01
MISL	40.59	27.59	1	1996.8-1996.8	−5.7	1.8	−15.3	1.9	−0.01
SOKE	37.82	27.49	2	1992.7-1996.8	−18.9	1.4	−19.8	1.4	−0.04

Table 1. (continued)

Site	Lat	Lon	No.[a]	Span[b]	N Vel	Nσ[c]	E Vel	Eσ[c]	ρ_{EN}[d]
				Eastern Mediterranean Sites (continued)					
BURG	42.67	27.44	2	1994.9-1996.8	−0.8	1.9	0.5	2.0	−0.01
ALAN	39.78	27.42	3	1990.7-1996.7	−9.6	1.4	−23.2	1.4	0.02
BODR	37.03	27.42	2	1994.7-1996.8	−25.3	1.3	−14.7	1.3	−0.03
KNID	36.68	27.39	2	1994.7-1996.8	−30.7	1.4	−9.0	1.4	−0.03
YENB	40.81	27.39	4	1990.7-1996.7	−5.0	1.4	−4.5	1.4	0.03
YAYA	39.02	27.32	1	1994.7-1994.8	−13.7	1.2	−20.9	1.2	−0.03
BAYO	38.71	27.31	2	1992.7-1996.8	−15.0	1.1	−17.7	1.2	−0.04
KABI	40.38	27.30	3	1990.7-1994.8	−6.2	1.8	−17.9	1.8	0.08
EGMI	39.58	27.27	3	1990.7-1994.8	−6.1	2.0	−19.7	1.9	0.09
MATR	31.35	27.23	3	1996.8-1997.8	5.1	1.9	−2.8	2.3	−0.02
KRPT	35.49	27.22	3	1988.8-1996.8	−30.7	1.1	−11.5	1.3	−0.01
KIRE	39.90	27.22	3	1990.7-1994.8	−8.6	1.1	−19.3	1.2	−0.01
ARAK	40.17	27.21	3	1990.7-1994.8	−9.1	1.9	−19.4	1.9	0.07
D5DU	39.24	27.11	2	1992.7-1994.8	−11.8	2.6	−18.4	2.6	0.00
SAMO	37.78	26.99	4	1988.8-1996.8	−24.3	1.1	−19.3	1.2	−0.01
KOSI	36.75	26.93	3	1988.8-1996.8	−27.0	1.1	−16.5	1.2	−0.01
BAHA	40.03	26.91	3	1990.7-1994.8	−8.9	1.9	−19.4	1.9	0.08
SEVK	40.40	26.88	4	1990.7-1994.8	−6.7	1.8	−17.2	1.7	0.05
KVAK	40.60	26.87	3	1990.7-1994.8	−4.4	1.9	−13.3	1.8	0.09
AYVA	39.33	26.71	4	1990.7-1996.7	−10.6	1.3	−20.1	1.4	−0.01
DOKU	40.74	26.71	4	1990.7-1996.7	−3.3	1.3	−4.0	1.3	0.00
AYKA	39.31	26.70	3	1992.7-1996.8	−12.2	1.2	−18.5	1.2	−0.03
LESV	39.23	26.45	3	1989.8-1996.8	−13.2	1.1	−20.5	1.2	−0.01
ASTP	36.59	26.41	3	1988.8-1996.8	−30.5	1.1	−14.9	1.2	−0.02
CEIL	38.31	26.39	3	1992.7-1996.8	−22.8	1.2	−17.1	1.2	−0.05
EZIN	39.78	26.32	3	1990.7-1994.8	−9.9	2.0	−19.0	1.9	0.04
KRKE	39.73	26.22	3	1990.7-1994.8	−10.9	1.9	−20.2	1.9	0.06
ZAKR	35.13	26.21	3	1988.8-1996.8	−28.4	1.1	−15.8	1.3	−0.01
BDER	39.61	26.19	3	1990.7-1994.8	−10.1	1.9	−18.2	1.9	0.03
SUBA	39.97	26.17	3	1992.7-1996.8	−10.5	1.1	−16.0	1.2	−0.04
KEST	39.73	26.16	3	1990.7-1994.8	−9.6	1.9	−19.6	1.9	0.03
HIOS	38.44	26.08	3	1989.8-1996.8	−23.4	1.1	−19.8	1.2	0.00
AMAN	39.50	26.08	3	1990.7-1994.8	−9.1	2.0	−19.2	2.0	0.04
ALEX	40.84	25.88	2	1994.9-1996.8	−7.7	2.0	−0.4	2.1	−0.03
ASKT	40.93	25.57	3	1992.4-1996.8	−2.6	1.3	0.0	1.3	−0.02
SMTK	40.47	25.51	2	1992.4-1996.8	−4.0	1.3	−3.1	1.4	−0.01
THIR	36.35	25.44	3	1988.8-1996.8	−31.0	1.1	−16.4	1.2	0.01
MKN2	37.45	25.38	2	1992.4-1996.8	−26.4	1.3	−16.6	1.4	−0.03
LIMN	39.85	25.13	3	1989.8-1996.8	−13.4	1.1	−15.5	1.2	0.00
ROML	35.40	24.69	5	1988.8-1996.8	−26.9	1.1	−16.5	1.2	−0.04
THAS	40.59	24.63	3	1989.8-1996.8	−3.2	1.1	−1.4	1.3	0.02
NSKR	38.89	24.54	3	1989.8-1996.8	−24.0	1.1	−12.6	1.2	0.00
MILO	36.75	24.52	3	1988.8-1996.8	−25.2	1.1	−16.4	1.2	−0.03
KYNS	37.36	24.41	3	1988.8-1996.8	−26.2	1.1	−17.6	1.2	−0.02
SEVA	38.09	24.39	4	1988.8-1996.8	−25.9	1.1	−15.9	1.1	−0.02
SKAL	41.38	24.24	3	1989.8-1996.8	−2.6	1.1	0.3	1.3	0.03
GVDO	34.84	24.07	2	1993.8-1994.7	−30.3	3.2	−16.1	3.1	−0.03
DIOC	38.08	23.93	4	1988.8-1997.8	−26.2	0.9	−15.7	0.9	−0.05
OMAL	35.33	23.93	4	1988.8-1996.8	−24.7	1.1	−16.6	1.3	0.01
STHN	39.99	23.92	3	1989.8-1996.8	−10.2	1.1	0.6	1.2	0.00
SOXO	40.79	23.43	3	1989.8-1996.8	−5.6	1.1	−0.9	1.2	0.03
PLAN	42.48	23.42	3	1994.9-1994.9	−2.8	1.4	−2.5	1.5	−0.01
KYRA	36.31	22.98	5	1988.8-1996.8	−25.6	1.1	−15.7	1.2	0.01
NEVA	38.89	22.94	3	1989.8-1996.8	−15.0	1.1	−8.7	1.2	0.01
LEON	37.18	22.82	3	1988.8-1996.8	−28.4	1.1	−16.8	1.2	0.03
KRNA	39.94	22.54	3	1989.8-1996.8	−7.4	1.3	1.4	1.4	−0.01
XRIS	36.79	21.88	5	1988.8-1996.8	−23.8	1.1	−18.2	1.2	0.04
LOGO	37.67	20.80	3	1993.8-1996.7	−22.6	1.6	−10.2	1.6	−0.03
KRTS	39.73	20.67	6	1989.8-1996.8	−3.1	1.1	−1.5	1.2	0.00
VASI	38.61	20.57	2	1993.8-1996.7	−7.6	1.6	−3.6	1.6	−0.03
ASSO	38.37	20.55	2	1993.8-1994.7	−8.5	3.4	−1.0	3.1	−0.04
GAIO	39.19	20.19	3	1993.8-1996.7	2.3	1.6	−4.1	1.6	−0.03
PNTN	39.75	19.86	2	1994.7-1996.7	4.1	2.3	−4.8	2.2	−0.05

Table 1. (continued)

Site	Lat	Lon	No.[a]	Span[b]	N Vel	Nσ[c]	E Vel	Eσ[c]	ρ_{EN}[d]
Eastern Mediterranean Sites (continued)									
OTHO	39.86	19.38	3	1993.8-1996.7	3.6	1.7	−1.7	1.6	−0.04
SPEC	40.06	18.46	3	1993.8-1996.7	4.70	1.6	8.7	1.6	−0.03
Eurasian and Central Asian Sites Used to Define Eurasian Fixed Reference Frame									
POL2	74.69	42.68	c	1995.4-1999.2	2.1	0.9	1.5	1.0	−0.02
KIT3	66.89	39.13	c	1994.8-1999.0	1.4	0.9	0.5	1.0	−0.06
ZWEN	36.76	55.70	c	1995.4-1999.2	0.6	1.0	0.4	1.2	−0.01
METS	24.40	60.22	c	1992.7-1999.2	−0.8	0.9	−0.1	0.9	0.01
JOZE	21.03	52.10	c	1994.2-1999.2	−1.1	0.8	0.4	0.7	0.00
TROM	18.94	69.66	c	1988.8-1999.1	0.3	0.8	−0.6	0.9	0.01
BOR1	17.07	52.28	c	1994.7-1999.2	−0.1	1.1	−0.7	1.1	0.00
GRAZ	15.49	47.07	c	1992.7-1999.2	−0.1	0.9	0.6	0.9	0.00
POTS	13.07	52.38	c	1994.8-1999.2	−0.2	1.1	0.0	1.1	0.00
WTZR	12.88	49.14	c	1991.6-1999.2	0.7	0.8	0.2	0.8	0.02
ONSA	11.93	57.40	c	1988.8-1999.2	0.0	0.8	−1.4	0.8	0.03
NYAL	11.86	78.93	c	1991.1-1999.2	0.7	0.8	1.6	0.8	0.09
ZIMM	07.47	46.88	c	1994.2-1999.2	−0.9	1.0	0.7	1.0	0.03
KOSG	05.81	52.18	c	1991.1-1999.2	0.1	0.8	−0.1	0.9	0.03
BRUS	04.36	50.80	c	1994.4-1999.2	−0.1	1.0	−0.6	1.0	0.03
HERS	00.34	50.87	c	1992.7-1999.2	−0.7	1.2	−0.2	0.7	0.04

Latitude (Lat) and Longitude (Lon) are given in degrees north and east, respectively. Station velocities (Vel) and their uncertainties are given in mm/yr. The Eurasian frame is determined by minimizing the adjustments to the horizontal velocities of the 16 stations given at the end of the table. A priori velocities for all of the European stations were set to zero, while the central Asian stations (POL2 and KIT3) were assumed to have an a priori velocity of 2 mm/yr N and 0.5 mm/yr E to account for their measured motion with respect to the Kazakh platform [T. Herring, personal communication, 1999].

[a]Number of observation epochs. Continuous stations are denoted with c.

[b]Observation time span. Dates are given in tenths of years.

[c]1 sigma uncertainties.

[d]Correlation coefficient between the east and north uncertainties.

tween June 1992 and April 1999. The global solutions were performed by the Scripps Orbit and Permanent Array Center (SOPAC) [*Bock et al.,* 1997; solutions available at http://lox.ucsd.edu]. Altogether, our solution includes data spanning 9 years from 450 stations, including 189 in the Mediterranean region.

We analyzed the data using the GAMIT/GLOBK software [*King and Bock,* 1998; *Herring,* 1998] in a three-step approach described by *Feigl et al.* [1993], *Oral* [1994], and *Dong et al.* [1998]. In the first step, we used doubly differenced GPS phase observations from each day to estimate station coordinates, the zenith delay of the atmosphere at each station, and orbital and Earth orientation parameters (EOP), applying loose a priori constraints to all parameters. This analysis included data from three to four IGS stations used to link the regional and global networks. In the second step we used the loosely constrained estimates of station coordinates, orbits, and EOP and their covariances from each day as quasi-observations in a Kalman filter to estimate a consistent set of coordinates and velocities. In this step we combined for each day the quasi-observations from our regional analysis with the quasi-observations of a global analysis of IGS data performed by SOPAC. For convenience and to better assess the long-term statistics of the measurements we then combined the daily estimates (quasi-observations) into a single set for each survey. At times when there were no regional observations we combined the daily quasi-observations from the SOPAC analysis of the IGS global data into monthly averages. We determined the weights for each set of quasi-observations by averaging the increments in chi-square per degree of freedom from a forward and backward filtering of the data.

The reference frame for our velocity estimates was defined only at the third step, in which we applied generalized constraints [*Dong et al.,* 1998] while estimating a six-parameter transformation (six components of the rate of change of translation and rotation). Specifically, we defined a Eurasian frame by minimizing the horizontal velocities of 16 IGS stations in western Europe and central Asia (Table 1). The root-mean-square (rms) departure of the velocities of the 16 stations after transformation was 0.6 mm/yr. Given the small number of well-observed stations in Eurasia but outside of western Europe, we tested several alternative realizations of our

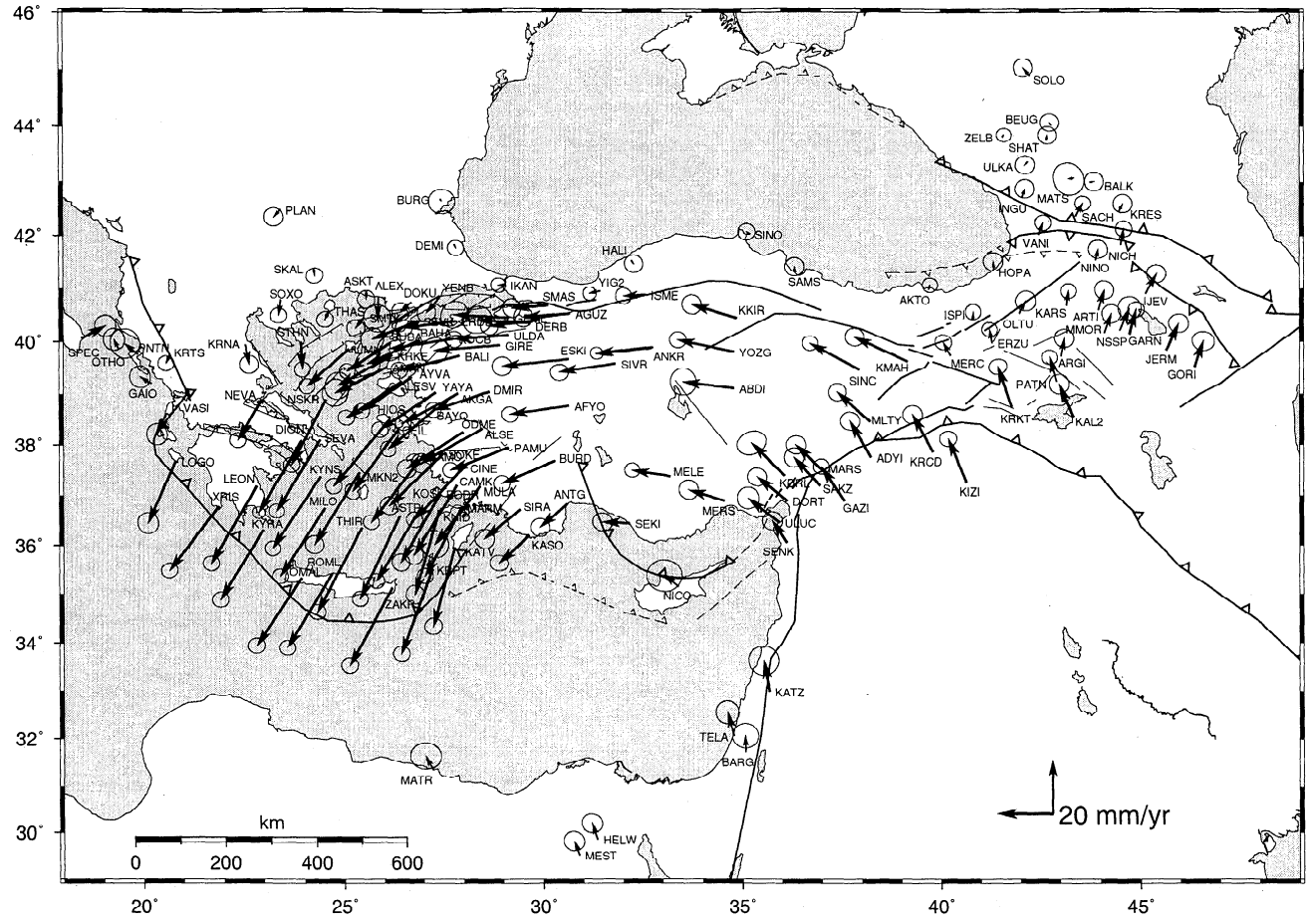

Figure 2. GPS horizontal velocities and their 95% confidence ellipses in a Eurasia-fixed reference frame for the period 1988–1997. To avoid clutter, we have omitted plotting some sites in the Marmara region, but in Table 1 we list velocities for all sites. Tectonic symbols are as in Plate 1.

reference frame using different subsets of stations. If we omit the two central Asian stations (KIT3 and POL2), for example, velocities in the Aegean shift 1 mm/yr SW and in eastern Anatolia shift 2 mm/yr SW. We also considered realizing a Eurasian frame by first minimizing the adjustment of the velocities of 40 globally distributed stations from a priori values given in the not-net-rotation (NNR) frame of the International Terrestrial Reference Frame (ITRF96) [*Boucher et al.*, 1998] and then rotating our estimated velocities to a Eurasian frame using the global plate model NUVEL-1A [*DeMets et al.*, 1994]. We rejected this approach, however, since although it produced a good global fit to ITRF96 (0.9 mm/yr), the rms of Eurasian stations was 3 mm/yr. With this ITRF96/NUVEL-1A realization of a Eurasian frame, velocities in the Aegean shift 2 mm/yr NE and in eastern Anatolia shift 4 mm/yr NE.

Velocities of stations in Turkey and the Caucasus with respect to Eurasia are shown in Figure 2 and listed in Table 1. The 1σ uncertainties for the GPS velocities were derived by scaling the formal errors by the square root of chi-square per degree of freedom of the solution, as discussed below. To better assess the real uncertainties, we computed time series of station position, using the same approach as for the velocity solution except that we treated each set of quasi-observations (survey or monthly averaged continuous observations) independently and defined the reference frame at each epoch by minimizing the adjustments of horizontal position for all stations from values estimated from the velocity solution. Figure 3 shows the detrended residual time series for four stations which together represent results from each of the major surveys and the SOPAC analysis of continuous data. Dionysos (DIOC) was occupied for 9 days in the 1988 and for 8 days in the 1989 Aegean surveys, the 1992 Aegean survey, and the 1996 combined Aegean/Turkey survey. Zelenchukskaya (ZELB) was occupied for 14 days in the 1991 Caucasus survey, the 1994 and 1996 integrated eastern Mediterranean surveys, and the 1997 Caucasus survey. The large uncertainties (3–4 mm in north, 4–5 mm in east) for the early surveys are a result of the limited satellite constellation (and hence shorter occupation times)

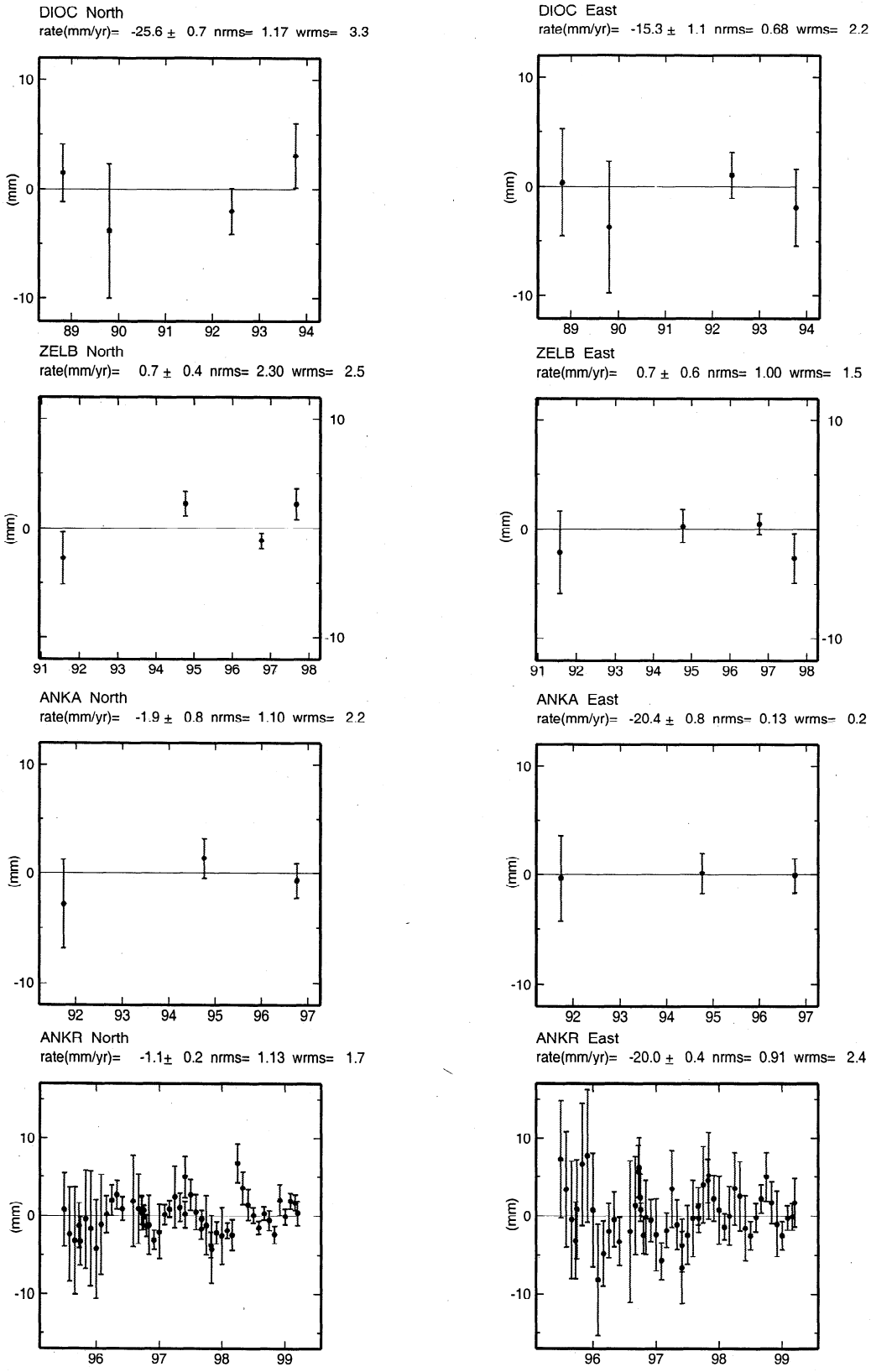

Figure 3. Time series of geocentric position of stations at Dionysos (DIOC) in southern Greece, Zelenchukskaya (ZELB) in the Caucasus, and Ankara (ANKA, ANKR) in Turkey, after removing the best fit straight line. Labels show estimated rate with respect to Eurasia, its 1σ uncertainty, and the normalized (nrms) and weighted (wrms, in mm) root-mean-square scatters. The uncertainties in rates shown with the plots reflect our scaling of the overall solution but not the random walk process noise added to the solution (see text); hence for the well-determined rates the uncertainties shown are smaller than those estimated in the velocity solution and given in Table 1.

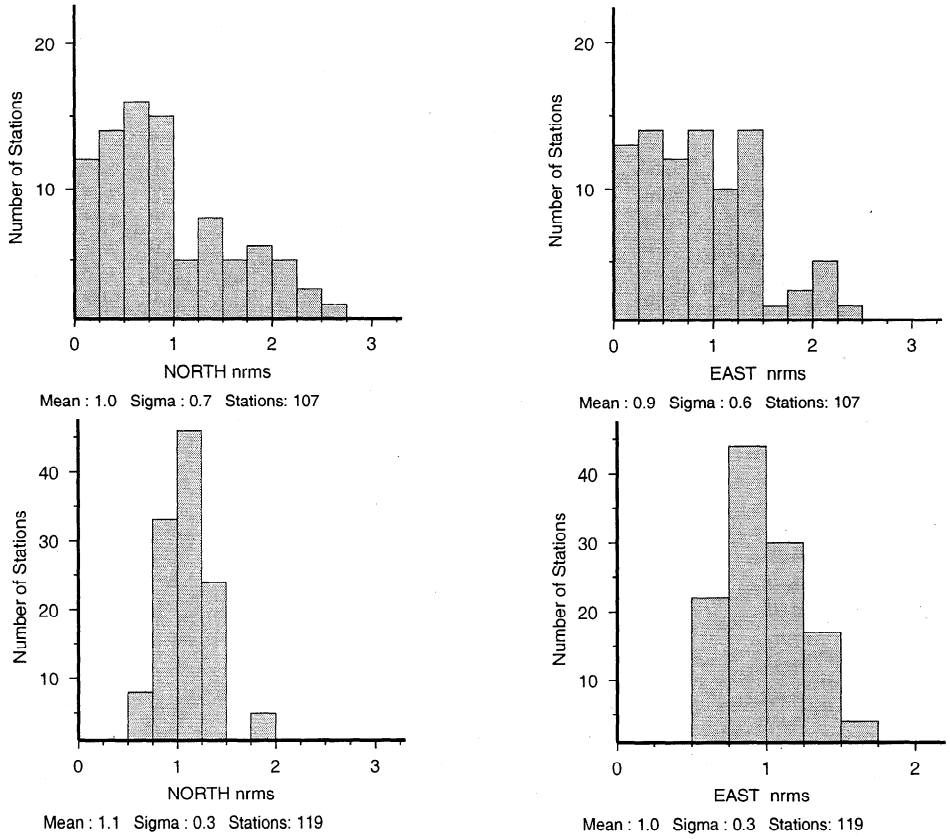

Figure 4a. Histogram of the normalized rms for (top) regional and (bottom) global stations with three or more measurements.

and global tracking network prior to 1992. At Ankara we occupied station ANKA for 3 days in four of the five most recent surveys and also used data from the continuous station ANKR from 1996 forward.

In Figure 4a we show histograms of the normalized rms (nrms, square root of chi-square per degree of freedom) for the regional and global stations with at least three measurements. The distribution of nrms values for the global stations, each with 18 or more (monthly averaged) measurements, is reassuringly Gaussian with a mean close to 1.0. The distribution for regional stations, most with only three or four measurements, is quite irregular. The excess of small values results from many stations having only three measurements, the earliest of which carries low weight, allowing a straight line to be fit nearly perfectly to the other two. The excess of large values indicates unwelcome outliers that will lead to an underestimate of the velocity uncertainties for these stations. With only two or three measurements we usually cannot identify the outliers. To provide additional insight into the overall quality of the analysis, we show in Figure 4b the distribution of weighted rms values. The means for the regional stations are <3 mm and for the global stations are 3 mm in north and 4 mm in east.

Scaling the velocity uncertainties by the square root of chi-square per degree of freedom from the solution would be appropriate if the error spectrum were white and spatially homogeneous. It is clear from the time series for ANKR (Figure 3), however, that there are significant errors with correlation times greater than the duration of each survey. Recent analyses of continuous data by *Zhang et al.* [1997] and *Mao et al.* [1999] indicate that the noise in GPS time series may be characterized by colored noise with a spectral index which varies from about 0.5 (fractal white noise) to 1.5 (fractal random walk) depending on the station and the method of analysis. Time series of geocentric station position tend to show significant quasi-annual and other long-period components whose origins are still unclear but which are presumably related to mismodeling of the troposphere or motions of the satellites (see ANKR in Figure 3 and the global time series of *Mao et al.* [1999]). By removing a common mode component within a region, however, as *Zhang et al.* [1997] do explicitly and we do implicitly in estimating relative velocities, we reduce the magnitude of these effects and whiten the noise. We tested the effect of correlated noise in our analysis by performing four different solutions, one in which the errors in station position estimates were assumed to be random and three in which we added a random walk component equal to 1, 2, or 3 mm/$\sqrt{}$yr. The random component is determined by the inherent strength of the survey and the reweighting we applied based on its

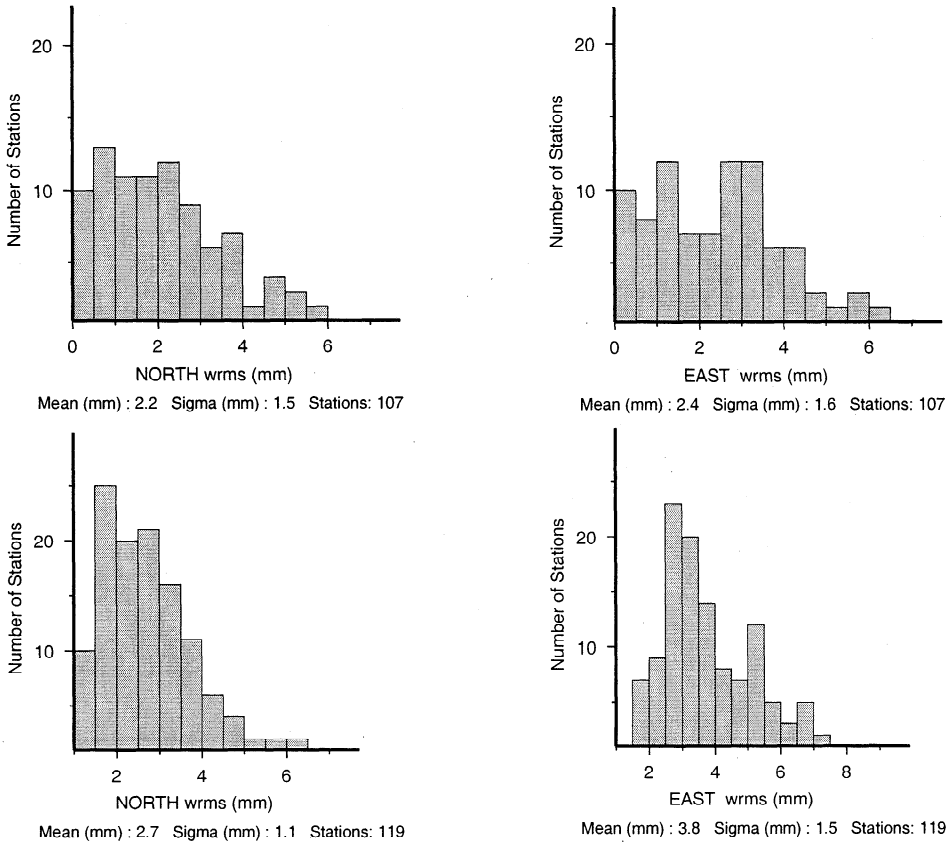

Figure 4b. Same as Figure 4a but for weighted rms (in mm).

consistency with other surveys (chi-square increment in the combination) and varies from 7 mm for the early surveys to 2 mm for the most recent surveys and continuous data. We found that after scaling the estimates by the square root of chi-square for the solution (1.4 for the white noise case and 1.3, 1.1, and 0.8, respectively, for the three cases in which we added random walk) the differences in the uncertainties that we obtained for horizontal velocities were <20% for stations observed annually or observed continuously for at least 4 years. As expected, the stations for which adding a random walk component has the largest effect on uncertainty are those observed continuously for only a short time, in our case, NICO on Cyprus, and KATZ in Israel. In order to represent the uncertainties of these stations more realistically and also to account for a possible random walk component due to monument instability [*Langbein and Johnson,* 1997], we have chosen to present the solution in which we allowed a random walk of 2 mm/$\sqrt{\text{yr}}$ in horizontal positions of the stations.

An important limitation of assigning velocity uncertainties based on the time series is that this analysis poorly resolves the most important components of the error, those with temporal scales comparable to the time span of the measurements. Hence, whenever possible, we should evaluate our estimates of uncertainty by applying external knowledge that does not depend on knowing the full character of the error spectrum. For the eastern Mediterranean analysis we did this by examining at different levels of confidence the residuals of 28 stations in four regions which have relatively little internal deformation: southern Eurasia west of E35°, central Anatolia, the south central Aegean, and northern Arabia. For these 28 stations the relative velocity residuals of 11 stations fell outside the error ellipses of 50% confidence, 5 outside 80% confidence, and 3 outside 95% confidence. Given the limitations of small-number statistics and the possibility that some of the excess residual is due to actual deformation, we believe that this result corroborates our error model. In Table 1 and in the text we give uncertainties as one standard deviation after scaling; in the figures we plot regions of 95% confidence.

3. Discussion

3.1. Description of the Velocity Field and Regional-Scale Motions

The GPS velocity field shown in Figure 2 quantifies the northward motions of northeastern Africa as well as the northern part of the Arabian plate and the

counterclockwise rotation of much of central/western Turkey and the southern Aegean/Peloponnisos. This rotation is bounded to the north by the NAF and its extension into the north Aegean Sea (i.e., north Aegean trough). East of the Karliova triple junction (~41°E longitude) the character of broad-scale motion changes abruptly. Motions in eastern Turkey show progressively more easterly directions toward the NNE, resulting in shortening more or less normal to the Caucasus thrust front in Armenia and Georgia. To first order, continental material north of the Arabian-Anatolian plate collision zone (Bitlis suture) appears to move around and between the oceanic lithosphere of the Black and Caspian Seas, the Anatolian plate moving to the west and eastern Turkey/Caucasus moving around the eastern side of the Black Sea.

The GPS velocities for sites located well south of the Bitlis suture on the northern edge of the Arabian plate (KIZI, KRCD, GAZI) indicate NW oriented motion relative to Eurasia (18 ± 2 mm/yr oriented N24°$\pm$ 5°W; 16 ± 2 mm/yr oriented N32°$\pm$ 5°W; and 15 ± 2 mm/yr oriented N40°$\pm$ 5°W, respectively), less than NUVEL-1A estimates (25 ± 1 mm/yr oriented N21°$\pm$ 7°W at KIZI). The slower GPS rates may indicate that stations along the northern edge of Arabia are involved in the Arabia-Anatolia deformation and/or that crustal shortening occurs within the Arabian plate to the south, possibly in the Palmyrides [e.g., *Chaimov et al.,* 1990]. Alternatively, this discrepancy might indicate slowing of the Arabian plate during the recent geologic past, or uncertainties in NUVEL determinations of plate motions in this region which are based on global plate circuit closures and distant spreading centers [*DeMets et al.,* 1990]. A better understanding of the possible contributions of these effects will require improved long-term plate motion estimates and improved geodetic control over a larger part of the Arabian plate interior.

The two stations located on the northeastern edge of the African plate (HELW and MEST) were observed over only a 3-year period (Table 1), and accordingly, the reported motions are less reliable. These stations show northward motion in a Eurasia-fixed frame at rates of 6 ± 2 and 5 ± 2 mm/yr, respectively. This is about a factor of 2 less than the rate determined by NUVEL-1A (10 ± 1 mm/yr at N2°$\pm$ 4°E). Station MATR in western Egypt has too high an uncertainty ($\pm$ 4 mm/yr) to provide a useful constraint on Africa plate motion. Station BARG, located close to the Dead Sea transform in Israel, shows northward motion at a rate of 7 ± 3 mm/yr, closer, but still below, the rate anticipated for Africa from NUVEL-1A (11 ± 1 mm/yr oriented N2°$\pm$ 3°E). These slow present-day rates for northeastern Africa are supported by satellite laser ranging (SLR) observations near HELW and BARG [*Robbins et al.,* 1995], but the SLR results have high uncertainties at these locations (Helwan, 6 ± 9 mm/yr at 213°$\pm$ 62°; Bar Giyyora, 9 ± 3 mm/yr at 12°$\pm$ 53°). The significance of these observations for overall African plate motion is difficult to determine because of possible effects of the Dead Sea fault and/or the Sinai microplate [e.g., *Courtillot et al.,* 1987]. While the present data suggest possible motions across the Gulf of Suez [*Joffe and Garfunkel,* 1987] and the Sinai block (i.e., between HELW/MEST and BARG/TELA), additional GPS observations are needed to confirm both the preliminary slow rate for NE Africa and possible motion of the Sinai block relative to Africa.

Stations located in northern Greece, Bulgaria, north of the NAF in Turkey, and north of the Caucasus show insignificant or small motions in the Eurasia-fixed reference frame. There is weak evidence for possible N-S extension north of the north Aegean Sea (SOXO, STHN), consistent with seismic and neotectonic observations [*Voidomatis et al.,* 1990].

3.2. Crustal Deformation and Strain Partitioning in Eastern Turkey and the Caucasus

The velocity field shown in Figure 2 (see also Figures 5 and 6) suggests that the northwestward motion of Arabia is transferred directly to the region of eastern Turkey north of the Bitlis suture. As illustrated in Figure 5, east of the Karliova triple junction, GPS velocities tend to rotate progressively to the east at larger distances from the Bitlis suture, resulting in convergence approximately normal to the Greater Caucasus mountain front (e.g., see progressive change from KAL2, PATN, ARGI, GARN, IJEV). This rotation has been interpreted as evidence for distributed right-lateral, strike-slip faulting on northwest striking faults [*Reilinger et al.,* 1997b] in accordance with a model proposed by *Jackson* [1992]. Total convergence across the central and western Caucasus, best illustrated by stations located along the southern edge of the Lesser Caucasus in Armenia (ARTI, MMOR, GARN, JERM, GORI), is about 10 ± 2 mm/yr. This is about a factor of 3–10 higher than can be accounted for by earthquakes, indicating substantial aseismic deformation [e.g., *Jackson and McKenzie,* 1988; *Philip et al.,* 1989; *Reilinger et al.,* 1997b; *Jackson and Ambraseys,* 1997]. The partitioning of shortening between the Lesser and Greater Caucasus can be estimated from stations located in the intermountain valley separating the ranges, including VANI, NINO, and NICH. These stations have a NE velocity of between 5 and 6 ± 2 mm/yr, suggesting that ~60% of the shortening occurs within the Greater Caucasus.

The GPS results provide direct constraints on left-lateral fault slip along a NE-SW striking fault system in eastern Turkey and its proposed extension traversing the Greater Caucasus (see Figure 5; North East Anatolian fault (NEAF) in Turkey; Borjomi-Kazbeg (B-K) fault in the Caucasus). The nature of this fault system is particularly important since significant, throughgoing, left-lateral faulting oriented at an oblique angle to the Caucasus thrust front has been postulated in "in-

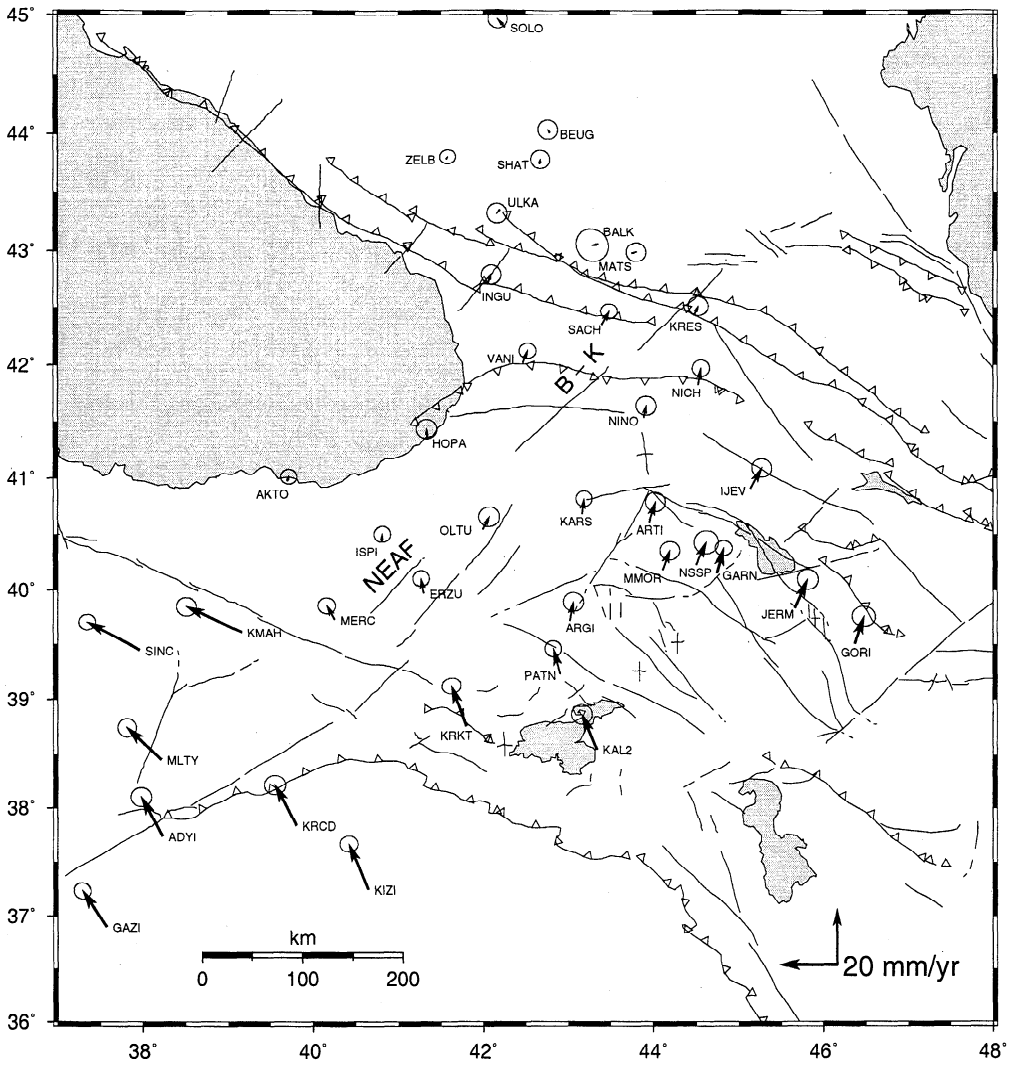

Figure 5. Expanded view of the GPS velocities for eastern Turkey and the Caucasus and their 95% confidence ellipses in a Eurasia-fixed reference frame superimposed on a map of active faults from *Avanessian and Balassanian* [1998]. Tectonic symbols are as in Plate 1. B-K, Borjomi-Kazbeg fault.

denter" models for the Arabia-Eurasia collision [e.g., *Philip et al.*, 1989; *Rebai et al.*, 1993; *Cisternas and Philip*, 1997]. *Jackson* [1992] proposes an alternative model which emphasizes partitioning of oblique convergence between right-lateral, strike-slip faulting on NW-SE striking faults in the south and shortening perpendicular to the Caucasus thrust front in the north. While the GPS results shown in Figure 5 allow some left-lateral motion along the NEAF system (e.g., between stations OLTU/KARS and HOPA/AKTO), stations within the Lesser and Greater Caucasus do not support the presence of significant left-lateral faulting on the B-K fault (e.g., between NINO, NICH, and VANI).

Using four stations on the Arabian plate (GAZI, KIZI, KRCD, shown in Figures 5 and 6 and the IGS station BAHR at 26.2°N, 50.6°E), we calculate a preliminary GPS Euler vector for Arabia-Anatolia (Table 2). Figure 6 shows the velocity field for eastern Turkey and the Caucasus rotated into the Arabia-fixed reference frame using the derived GPS Euler vector. This perspective illustrates the left-lateral, strike-slip nature of the Eastern Anatolian fault (EAF) and the northernmost end of the Dead Sea fault (DSF) (MLTY, KDRL, DORT, SENK). The station at Bar Giorra in Israel (BARG) supports left-lateral slip on the southern DSF. Stations in easternmost Turkey indicate that right-lateral deformation associated with the NAF extends east of the Karliova triple junction (KTJ), a hypothesis made independently on the basis of seismic and regional tectonic studies [*Westaway*, 1990; *Jackson*, 1992]. The fit between the small circle about the estimated pole and the EAF as mapped on the ground is rather poor but is perhaps expected given

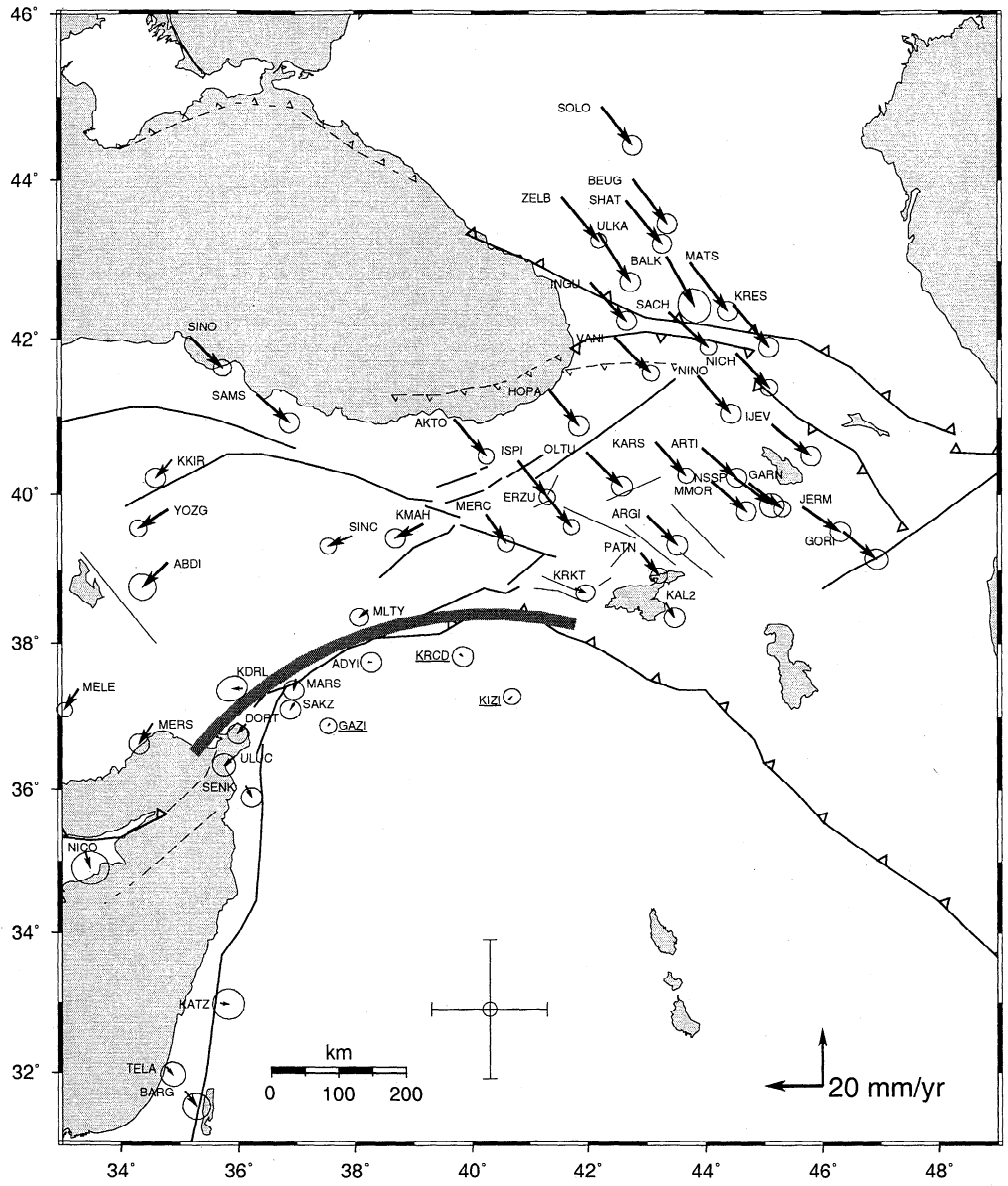

Figure 6. GPS horizontal velocities and their 95% confidence ellipses in an Arabia-fixed reference frame. Underlined stations were used to invert for the Arabia-Anatolia Euler vector (Table 2 and text). The pole and its 1σ uncertainties in north and east are shown near 33°N, 40°E. The arc is a small circle about this pole at the approximate location of the East Anatolian fault. Tectonic symbols are as in Plate 1.

the complex surface expression and seismic character of the fault [e.g., *Lyberis et al.*, 1992] (Figure 1). Stations ULUC and DORT near the EAF-DSF junction show motions similar to those expected for stations on the Anatolian plate, while station SENK is consistent with African plate motion, implying that the present Anatolian-African plate boundary (i.e., Cyprus Arc) comes on-land between ULUC and SENK and that the triple junction lies just north of SENK. These kinematics require significant left-lateral slip on the northern Dead Sea fault in contrast to some earlier interpretations [e.g., *Butler et al.*, 1997].

Following the model of *Jackson* [1992], *Reilinger et al.* [1997b] used the NUVEL-1A Arabia-Eurasia Euler vector to estimate Arabia motion just south of the Lesser Caucasus (GPS station GARN) and compared this to the observed GPS motion at GARN to determine the partitioning of strain between right-lateral deformation in eastern Turkey and shortening in the Caucasus. They argue that the difference between these motions represents the integrated deformation between the Bitlis suture and the Lesser Caucasus. We reexamine this conclusion using the improved velocity field and the GPS Euler vector from our current study. This Euler vector

Table 2. Euler Vectors for Anatolia-Eurasia (An-Eu), Arabia-Eurasia (AR-Eu), Anatolia-Arabia (An-Ar), Aegean-Eurasia (Ae-Eu), and Aegean-Anatolia (Ae-An)

Plate Pair	Lat, °N	Long, °E	Rate, Myr	Reference and Comments
An-Eu	30.7 ± 0.8	32.6 ± 0.4	1.2 ± 0.1	this study (A)
An-Eu	31.0 ± 0.8	31.8 ± 0.5	1.2 ± 0.1	this study (B)
An-Eu	14.6	34	0.64	*Jackson and McKenzie* [1984]
An-Eu	14.6	34	0.78	*Taymaz et al.* [1991]
An-Eu	31	35.5	0.83 ± 0.1	*Westaway* [1994a]
Ar-Eu	25.6 ± 2.1	19.7 ± 4.1	0.5 ± 0.1	this study
Ar-Eu	24.6 ± 1.6	13.7 ± 3.9	0.5 ± .05	*DeMets et al.* [1994]
An-Ar	33.1 ± 2.0	46.7 ± 2.4	0.7 ± 0.2	this study (NUVEL-GPS)
An-Ar	32.9 ± 1.3	40.3 ± 1.3	0.8 ± 0.2	this study (GPS-GPS)
An-Ar	−20.6	68.9	0.34	*Jackson and McKenzie* [1984]
An-Ar	−3.3	61.9	0.35	*Taymaz et al.* [1991]
Ae-An	38.0 ± 0.5	19.6 ± 1.2	1.2 ± 0.2	this study

Counterclockwise rotation is positive. Uncertainties are 1σ. This study (A) is vector A, determined using only stations in central Anatolia well away from active faults (Figure 8); this study (B) is vector B, derived using all stations in Turkey between the NAF and the EAF.

provides a better estimate of the motion of the northern part of Arabia relative to Eurasia than the NUVEL-1A vector since it is derived primarily from stations located just south of the Bitlis suture. The velocity for station GARN in Figure 6 (16 ± 1 mm/yr oriented N55°±5°W) is determined in precisely this way (i.e., by subtracting the predicted Arabian plate motion at this location from the observed GPS velocity). Within the uncertainties the velocity of GARN in Figure 6 has the same orientation as the average strike of right-lateral faults in the region [*Jackson,* 1992] (Figure 1), supporting and quantifying *Jackson*'s [1992] hypothesis that the northwestward motion of Arabia is partitioned between pure right-lateral strike-slip in eastern Turkey and pure thrusting along the Caucasus mountains.

3.3. Coherent Rotation of the Anatolian Plate

We describe the observed anticlockwise rotation of central Anatolia with respect to Eurasia in terms of an Euler vector for the relative motion. In estimating the Euler vector we investigated a number of possible least squares inversions of the horizontal GPS station velocities by including various combinations of stations. In Table 2 we give two such Euler vectors: Vector A is determined using only stations in central Anatolia well away from active faults (Figure 7); vector B is derived using all stations in Turkey between the NAF and the EAF. The difference in the Euler vectors is insignificant, demonstrating that, to first order, much of Turkey south of the NAF moves as a coherent unit with little internal deformation (excluding stations near the NAF and EAF which are within the elastic strain fields of these faults). Figure 7 shows residual velocities for GPS stations after removing the coherent plate motion for the An-Eu(A) Euler vector. A small circle about the pole at the approximate location of the NAF is also shown in Figure 7. In essence, Figure 7 shows the eastern Mediterranean velocity field in a reference frame fixed to the Anatolian plate.

The small circle in Figure 7 shows a good fit to the NAF in central Turkey but deviates from the mapped surface fault along its western segment (27°–34°E), including the Marmara Sea region, and the easternmost segment (39°–41°E). Both surface mapping and earthquake focal mechanisms indicate that the NAF becomes more complex (bifurcating into a number of active strands) with both strike-slip and extensional mechanisms west of about 31°E (Figure 1) [*Barka and Kadinsky-Cade,* 1988; *Barka,* 1992, 1997]. This change in character of the fault, which contrasts markedly with the simple, strike-slip behavior in central Turkey, is consistent with the mismatch between the idealized plate boundary represented by the small circle and the surface trace of the NAF. The difference in orientation between the strike of the small circle and the surface trace of the fault between 31° and 34°E in western Turkey and between 39° and 41°E in eastern Turkey implies that these fault segments should be in compression. This interpretation is supported by earthquake focal mechanisms (e.g., 1968 Bartin earthquake [*Alptekin et al.,* 1986]), high topographic relief (Plate 1) and thrusting and folding in the Quaternary basins adjacent to the fault zone along these segments of the fault [*Barka and Hancock,* 1984].

Residual velocities for stations located in the central part of Anatolia, east of 31°E, indicate that internal deformation in central Anatolia is <2 mm/yr. This and the low level of earthquake occurrence (Figure 1),

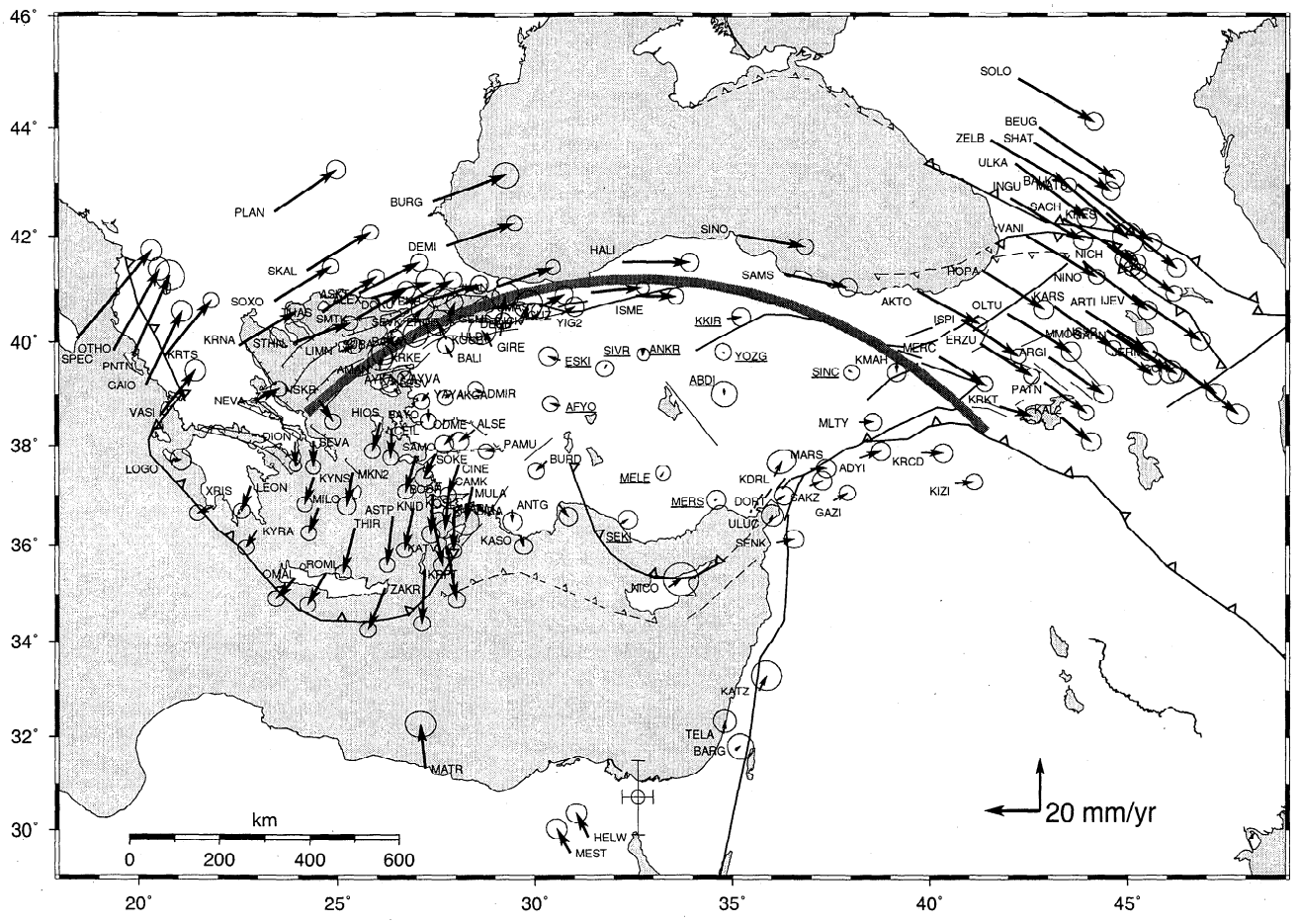

Figure 7. GPS horizontal velocities and their 95% confidence ellipses in an Anatolia-fixed reference frame (solution A, see text). Underlined stations were used to invert for the Anatolia-Eurasia Euler vector. The pole and its 1σ uncertainties in north and east are shown near 31°N, 32°E. The arc is a small circle about the pole at the approximate location of the North Anatolian fault. Tectonic symbols are as in Plate 1.

indicate that a plate description for central Anatolia is appropriate since deviations from coherent behavior are less than ~10% of overall Anatolia-Eurasia motion (i.e., <2 mm/yr compared to ~20 mm/yr along the NAF). Significant residual velocities for stations located near the NAF and EAF, including those in the Marmara region, likely reflect elastic or distributed deformation associated with these plate boundaries.

Stations located west of about 31°E show significant motions relative to central Anatolia. These motions consist of a small westward motion which grades into N-S extension in western Turkey. The central southern Aegean shows an apparent clockwise rotation in this Anatolian-fixed reference frame (see section 3.4).

3.4. Motion of the Southern Aegean

The GPS velocity field for the southern Aegean is dominated by SW motion relative to Eurasia of about 30 ± 1 mm/yr (Figure 2). In addition, the southern Aegean is characterized by a low level of seismicity (Figure 1). To better illustrate possible deformation in the southern Aegean, and the motion of the southern Aegean relative to surrounding areas, we calculate an Euler vector for the southern Aegean with respect to Anatolia (Table 2) and determine residual velocities in and around this region (Figure 8). To first order, much of the southwestern Aegean south of latitude 39°N shows little internal deformation (<2 mm/yr). In addition, stations in the Peloponnisos (LEON, KYRA, XRIS) suggest that, to first order, this area is moving coherently with the Aegean, although there is marginally significant evidence for clockwise rotation of the Peloponnisos in the Aegean-fixed reference frame. Stations in the southeastern Aegean (KATV, KRPT, ASTP, KNID, THIR) indicate increasing velocities toward the trench and counterclockwise rotation, with KATV moving southeastward at 10 ± 1 mm/yr relative to the Aegean as a whole. This pattern of relative motion in the SE Aegean is supported by the occurrence of normal fault earthquakes within the Aegean plate north and west of KATV (Figure 1).

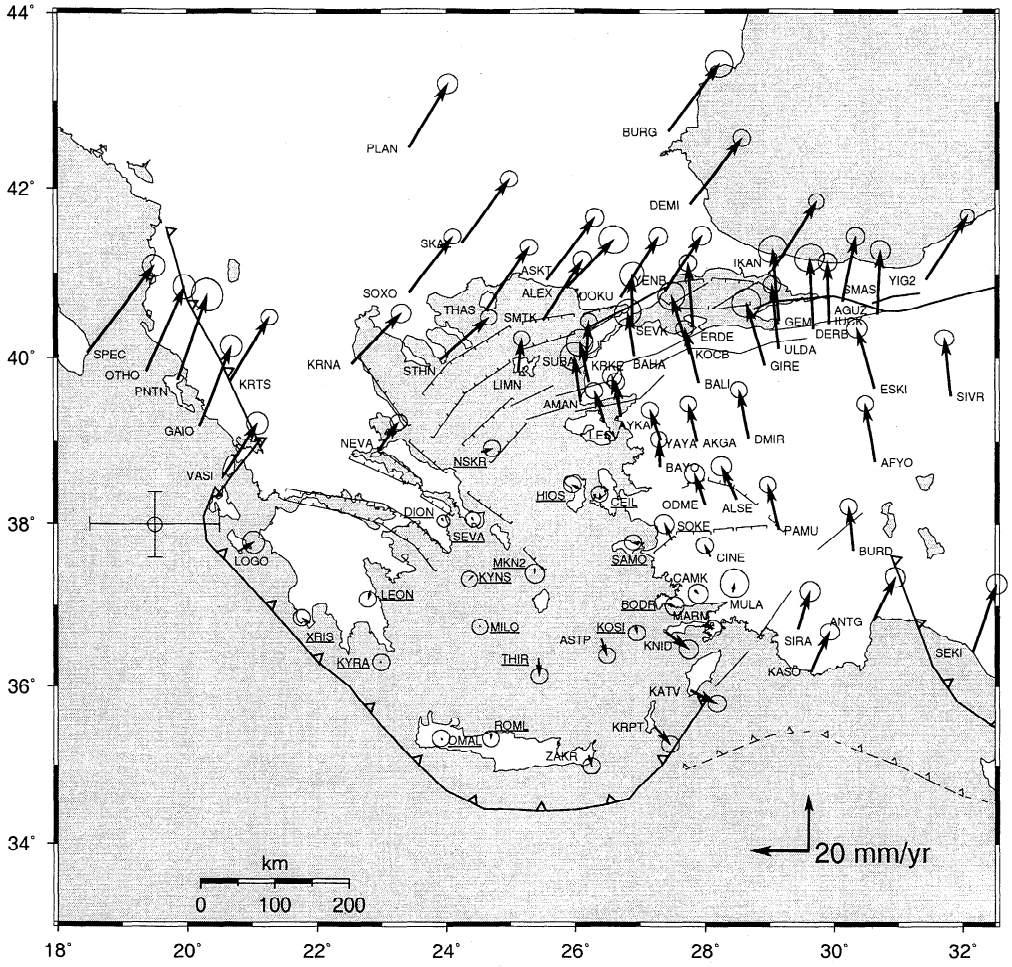

Figure 8. GPS horizontal velocities and their 95% confidence ellipses in a South Aegean-fixed reference frame (see text). Underlined stations were used to invert for the Aegean-Anatolian Euler vector (see text). Motion between the Aegean and Anatolia is distributed across western Turkey but, for the purpose of illustration, is shown as a bold NW-SE striking line. The rotation pole and its 1σ uncertainties in north and east are shown near 38°N, 20°E. Tectonic symbols are as in Plate 1.

3.5. Motion Between the Southern Aegean and Anatolia/Eurasia

Figures 7 and 8 illustrate, in two different perspectives, the relative motion between the Aegean and Anatolian regions and can be used to determine the approximate location of the Aegean-Anatolian "boundary." This boundary is indicated by the heavy solid line striking about N60°W in Figure 8. While the relative motion between the Aegean and Anatolia is distributed and not confined to a single fault, many of the strongest historic and recorded earthquakes in western Turkey occur near this location [*Ambraseys*, 1975, 1988] (Figure 1). GPS stations SW of this line show velocities more consistent with Aegean motion. Relative to Anatolia, these stations move roughly south (Figure 7). The velocity field suggests that southward motion is accommodated by the major E-W oriented normal faults associated with the horst and graben structures which dominate the active deformation in western Turkey (Buyuk Menderes and Gediz grabens, Plate 1). Using our estimated Aegean-Anatolian Euler vector, we determine a rate of motion between the Aegean and Anatolia which varies between 10 and 15 mm/yr.

Relative motion between the southern Aegean/Peloponnisos and Eurasia is concentrated in the northern Aegean Sea and along the Gulf of Corinth. Stations NEVA (38.9°N, 23.0°E) and NSKR (38.9°N, 24.5°E) have NE directed motions relative to the southern Aegean, consistent in orientation, but slower than stations on the Eurasian plate (Figure 8). This may imply that motion between the southern Aegean and Eurasia is distributed across the northern Aegean, an interpretation which is supported by the distribution of earthquakes (Figure 1). The character of earthquake focal mechanisms in the north Aegean indicates that this relative motion is accommodated by NE striking right-lateral strike-slip faults (i.e., deformation associated with the

extension of the NAF into the north Aegean) and NW striking normal faults (Figure 1).

The small or insignificant motions between the Peloponnisos and the southern Aegean (<1–2 mm/yr; i.e., <5% of Aegean-Eurasian motion) require considerable relative motion between the Peloponnisos and central Greece. This motion is apparently concentrated on E-W striking normal faults along the Gulf of Corinth, as indicated by earthquake focal mechanisms (Figure 1), more densely spaced geodetic studies [*Clarke et al.*, 1998], and neotectonic investigations [*Armijo et al.*, 1996]. In contrast, stations DION (38.1°N; 23.9°E) and SEVA (38.1°N; 28.4°E) appear to be moving along with the southern Aegean, requiring substantial relative motion between these stations and central Greece. It is not clear how this motion is accommodated [*Armijo et al.*, 1996], but a better understanding of this process could be critical for evaluating earthquake hazards in this highly developed area.

The Kephalonia fault zone (KFZ), (38.5°N, 20.5°E) takes up the motion between northwestern Greece and the Aegean-Peloponnisos region (Figure 2). It separates rapidly moving GPS stations on the central Ionian islands (e.g., LOGO) and the Peloponnisos (e.g., XRIS, LEON) from sites on the northern Ionian islands (GAIO) and NW Greece (KRTS), which show negligible motion relative to Europe. The dextral sense of strike-slip motion along the KFZ indicates an abrupt change in the Hellenic subduction zone [*Kahle et al.*, 1998].

In summary, the bulk of the motion of the southern Aegean/Hellenic arc appears to be associated with coherent rotation of the southern Aegean plate and is likely concentrated on SW striking, right-lateral strike-slip, and NW oriented normal faults in the northern Aegean Sea. Coherent rotation of the southern Aegean implies that contemporary extensional strain rates, and hence crustal thinning, in the Aegean region are considerably less than would be deduced by simply "distributing" the motion of the Hellenic arc across the region. Furthermore, the coherent, plate-like motions of Anatolia and the southern Aegean, separated by a zone of N-S extension in western Turkey, differs from *Reilinger et al.*'s [1997a] description of deformation based on more limited GPS data which suggested that the Anatolia-Aegean region could be approximated by a single plate deforming in the western region. The new data, particularly for the Aegean, show that a two-plate model, proposed by other investigators on the basis of seismic and neotectonic evidence [e.g., *McKenzie*, 1972; *Barka and Reilinger*, 1997] is a better description of the contemporary deformation field.

3.6. Slip Rates on the North Anatolian and East Anatolian Faults

While it is possible to estimate fault slip rates directly from the relative motions between GPS stations straddling the faults, more robust estimates can be derived for the NAF and EAF (i.e., Anatolia-Eurasia and Anatolia-Arabia boundaries) from the GPS Euler vectors. This procedure provides an upper bound on fault slip rate since we assume that all relative plate motion is accommodated on the main fault trace and make no allowance for possible accommodation on other faults or by anelastic deformation of the plates. In addition, this approach precludes examining possible variations in slip rate along the faults. On the basis of the Euler vectors given in Table 2 we estimate slip rates of 24 ± 1 mm/yr for the NAF and 9 ± 1 mm/yr for the EAF at the small circle radii plotted in Figures 7 and 6, respectively. The uncertainty in these estimates is due solely to the uncertainties in the Euler vector estimates and not the mislocation of the plotted small circles with respect to the actual fault traces. The estimated slip rate for the NAF is supported by independent GPS observations traversing the western end of the fault zone in the Marmara region which indicate total fault crossing rates relative to a station in Istanbul (and hence a lower bound) of about 20 ± 3 mm/yr [*Straub and Kahle*, 1994, 1995]. Historical slip rates based on seismic moments of earthquakes on the EAF are reported from 6 to 10 mm/yr [*Taymaz et al.*, 1991; *Westaway*, 1994a], again consistent with the rates indicated by the GPS results.

Our current estimates of rates for the NAF and EAF are both significantly lower than those given by *Reilinger et al.* [1997a] (30 ± 2 and 15 ± 3) based on an analysis of data from surveys between 1988 and 1994. The velocity estimates used to infer the Euler poles and fault rates of Reilinger et al. relied heavily on our analysis of data from the earliest surveys (1988–1990), which we now recognize was inconsistent with our analyses of the more recent data. For our current study we have reanalyzed the data from the 1991 and 1992 surveys and omitted the data from 1988–1990, which with the addition of the data from the 1996 survey would have little weight in the solution.

3.7. Relation Between Contemporary and Long-Term Geologic Deformation

We examine the relationship between present-day and long-term deformation to investigate possible implications of the GPS velocity field for the recent geologic evolution of the eastern Mediterranean region. Perhaps the best constrained long-term deformation is that associated with the NAF. *Sengor* [1979], *Barka and Kadinsky-Cade* [1988], *Barka* [1992, 1997], *Westaway* [1994a], and *Armijo et al.* [1999] present detailed geological and seismological descriptions, including estimates of slip rates, age of the current fault configuration, and total fault offsets. The throughgoing fault is constrained to be Pliocene in age (~4–5 Ma) with total offsets in the range of 80–100 km. This gives an average geologic slip rate of 16–25 mm/yr in good agreement with the GPS upper bound of 24 ± 1 mm/yr. The consistency between the GPS and geologic estimates, albeit within large uncertainties, supports the interpre-

tation that the NAF is Pliocene in age and that fault slip rates have not changed substantially since the fault initiated. The fit between the NAF and the small circle about the Euler pole and the absence of paleomagnetic rotations along the central and eastern NAF [*Platzman et al.,* 1994] are consistent with slip being primarily concentrated along a single fault. The consistent right-lateral, fault-parallel character of focal mechanisms for major earthquakes on the NAF (Figure 1) and the fact that all relative motion can be explained by seismic slip [*Jackson and McKenzie,* 1988] also argue against significant off-fault deformation (i.e., <5–10%) on the central NAF.

The left-lateral EAF has a much more complex surface expression than the NAF [e.g., *Lyberis et al.,* 1992; *Westaway,* 1994a]. It is thought to extend for ~500 km from the Karliova triple junction to some poorly defined location near the Gulf of Iskenderun where it apparently joins the northern end of the Dead Sea fault (Plate 1). The age of the fault is thought to be Pliocene (~4–5 Ma). Total left-lateral offset measured in the field has been estimated at 22 km by *Dewey et al.* [1986] and 27 km by *Arpat and Saroglu* [1972], indicating an average geologic slip rate of about 4–7 mm/yr, which may be compared to the GPS upper bound of 9 ± 1 mm/yr.

Geologic estimates of average extension rates in western Turkey and the Aegean are poorly constrained. *Sengor et al.* [1985] suggest that roughly 30% N-S extension has occurred across the western Turkey region. The onset of extension is thought to predate the initiation of the NAF and has been estimated as Miocene in age (~15 Ma), although some evidence suggests that extension may have intensified during the Pliocene (~5 Ma) [*Westaway,* 1994b]. This gives an average geological extension rate across SW Turkey (36.5° to 38.5°N) of 6–18 mm/yr, roughly consistent with the GPS Aegean-Anatolian motion of 10–15 mm/yr.

The absence of significant GPS strain in the central and southern Aegean and Peloponnisos seems difficult to reconcile with the generally thin crust (~24 km [*Makris,* 1978]) and high heat flow [e.g., *Stiros,* 1991] which characterize the Aegean back arc region. However, if back arc extension predates the initiation of the NAF as hypothesized [*Angelier et al.,* 1982; *Stein and Barka,* 1995; *Armijo et al.,* 1996], it is at least plausible that the southern Aegean was extended prior to NAF deformation propagating into the north Aegean. Propagation of the NAF into the north Aegean concentrated the more recent (~5 Ma) phase of extension in the northern Aegean and in the Gulf of Corinth, leaving the southern Aegean to translate SW as a coherent unit. The relatively young age inferred for the Gulf of Corinth (1 Ma [*Armijo et al.,* 1996]) is consistent with this scenario, and in fact, *Armijo et al.* [1996] suggest a similar evolution for the Aegean based on geologic investigation of the Gulf of Corinth and surrounding regions. In this same study they report that the principal fault bounding the Gulf of Corinth (Xylokastro fault) has absorbed ~7 mm/yr N-S extension over the past 350 kyr. Our GPS results indicate extension between NEVA and the Peloponnisos of 12 ± 1 mm/yr, which is in reasonable agreement with this longer-term average given that the GPS results integrate motions across much of central Greece.

Total shortening across the Greater Caucasus is uncertain with estimates reported in the range 5–60 km [*Dotduyev,* 1986; *Gamkrelidze and Gamkrelidze,* 1977]. *Triep et al.* [1995] point out that a minimum of 33 km of shortening is needed to account for present-day relief assuming Airy isostasy. The onset of convergence in the Greater Caucasus is estimated at 2.5 Ma [*Burtman,* 1989], although shortening may have begun as early as 5 Ma [*Triep et al.,* 1995]. Using this range of parameters (33–60 km shortening in 2.5 to 5 Myr) gives an average shortening rate in the range 7–24 mm/yr. In contrast, *Westaway* [1990] reexamined neotectonic information and concluded that overall shortening rates across the Greater Caucasus are likely no greater than ~5 mm/yr and that most of the convergence between Arabia and Eurasia is taken up to the south in eastern Turkey and northwestern Iran. Assuming uniform deformation rates, the GPS estimate of present-day shortening across the Greater Caucasus ($5–6 \pm 2$ mm/yr) supports *Westaway*'s [1990] analysis.

3.8. Implications for Lithospheric Rheology and Dynamics

Detailed knowledge of the kinematics of plate motions and interplate deformations is necessary but not sufficient to uniquely constrain the forces responsible for deformation. Inferences about the dynamics of contemporary deformation also require a knowledge of the rheology of the deforming lithosphere. While we can measure kinematics directly with geodetic observations, information on crustal and upper mantle rheology can only be deduced indirectly from laboratory studies and from seismic and other geophysical observations [e.g., *Thatcher,* 1995]. However, the kinematic information may help to eliminate certain classes of rheological models and dynamical processes and thereby help to identify those models which warrant more detailed investigation.

A principal result of this study is the coherent rotation and small internal deformation of the Anatolian and southern Aegean plates and the observation that the majority of motion between the Anatolian and Eurasian plates is confined to a relatively narrow fault zone (NAF) along a long section of the plate boundary. Another first-order result is the clear tendency for continental material to move around and between the oceanic lithosphere of the Black and Caspian Seas and the different styles of deformation east and west of the KTJ (distributed deformation and coherent plate motion, respectively). Also important for constraining dynamic processes is the increase in Anatolia plate velocity toward the west, and the rapid motion of the SE Aegean toward the Hellenic trench. Any model of

lithospheric rheology and dynamics for this region must account for these kinematic observations.

The observation that at least 90–95% of the motion of the Anatolian and southern Aegean plates can be explained in terms of coherent plate rotation requires either a relatively strong lithosphere or dynamic processes that result in small stresses over large distances (~500 km). Moreover, the primary deformation associated with both the Anatolia-Eurasia and Anatolia-Arabia boundaries is strike-slip, with little shortening even along the EAF. If the collision of Arabia is driving Anatolia plate motion, these kinematics require that the continental lithosphere of Anatolia is weaker under shear than compression. If Anatolia motion is primarily driven by flow in the mantle, the coherent motion of Anatolia and the southern Aegean still requires lithosphere that is strong relative to the underlying mantle; however, the arguments regarding the relative strength under compression and shear no longer apply.

The tendency for continental material to move around and between the oceanic lithosphere of the Black and Caspian Seas and the contrast in deformation style between the nondeforming Anatolian plate and the deforming eastern Turkey/Caucasus region are also important for constraining rheological models of the continental and oceanic lithosphere. The different styles of deformation could be due to a number of factors, including different rheological characteristics of the continental lithosphere east and west of Karliova, although the two areas seem to have had similar precollisional tectonic histories [e.g., *Zonenshain et al.,* 1990]. A simple explanation is the different boundary conditions imposed on these two areas. The westward motion and counterclockwise rotation of Anatolia is virtually unimpeded by the Hellenic trench. In fact, the observed increase in velocities toward the trench indicates that the Anatolian plate is being "pulled" by the foundering African plate or by mantle convection in the Aegean region [*Sonder and England,* 1989; *Royden,* 1993]. In contrast, eastern Turkey is apparently being driven against the strong oceanic lithosphere of the Black and southern Caspian Seas and the Eurasian continent which presumably serve to resist northward or eastward motion.

The apparently rigid character of the Black Sea oceanic lithosphere also provides a simple explanation for the deviation of the NAF from the small circle path in western Turkey. As indicated in Figure 7, the small circle passes through the SW corner of the Black Sea, while the NAF is deflected to the south. Perhaps this deflection results from the fault preferring to break weak continental crust rather than stronger oceanic crust. West of the Marmara Sea the main active branch of the NAF again steps north and is oriented parallel to the small circle path as evidenced by the GPS velocity field (Figure 7), historic earthquakes, and neotectonic observations [*Barka,* 1997]. The transfer of motion to the north branch of the western NAF may also account, in part, for the rapid, ongoing extension in the Marmara Sea and the more distributed nature of right-lateral shear in the northern Aegean.

In regard to the forces driving deformation, an important question for this area, as well as other tectonically active continental areas, is the relative importance of forces acting on boundaries between adjoining plates and those acting on the base of the plate (i.e., mantle flow or drag). Certainly, the increase in movement rates for the Anatolian plate toward the west and the more rapid southward motion of the Aegean require forces other than pushing on the edge of the plate by Arabia. If this added force is due to "pulling" by the foundering African plate along the Hellenic subduction zone, the coherent motion of much of the southern Aegean would seem to require that the plate be decoupled from the underlying mantle by a zone of weakness; otherwise, we might expect deformation to be concentrated along the edge of the plate. A weak zone decoupling the Anatolian plate from the underlying mantle also seems necessary to account for the coherent motion of this broad region if forces acting on the plate boundary are important for Anatolia motion. An alternate view is that all the observed motions reflect flow at depth which is deflected by the hard (and deep?) oceanic lithosphere to the north (Black and Caspian Seas). In this case, it still seems necessary to have a relatively strong continental lithosphere to account for the large areas of coherent motion.

The well-defined rapid trenchward motion of the SE Aegean contrasts with the absence of increasing motions toward the trench along the western and southern segments of the arc (Figure 8). While rapid trenchward motion supports the notion that forces associated with the subducted African plate are fundamentally responsible for ongoing motions and deformations in the Aegean, it is not obvious why the SE Aegean should show anomalously high rates of motion. We note that Africa-Aegean relative motion is approximately normal to the arc along the western arc and parallel to the arc along the eastern segment (Figure 2). Furthermore, it is reasonable to assume that slab geometry is complex at the high angle junction between the Hellenic and Cyprus arcs, although the detailed geometry of the downgoing slab has not yet been clearly delineated. A possible explanation, following the ideas of W. Spakman and coworkers [e.g., *Wortel and Spakman,* 1992], is that the rapid motions in the SE Aegean are a response to rapid sinking of the downgoing plate possibly associated with a tear at the Hellenic-Cyprus arc junction [*Barka and Reilinger,* 1997]. An alternate possibility is that the absence of compression along the eastern segment of the arc (Figure 1) allows the arc to more easily override the African plate.

4. Conclusions

GPS measurements for the period 1988-1997 provide a quantitative map of present-day plate motions and

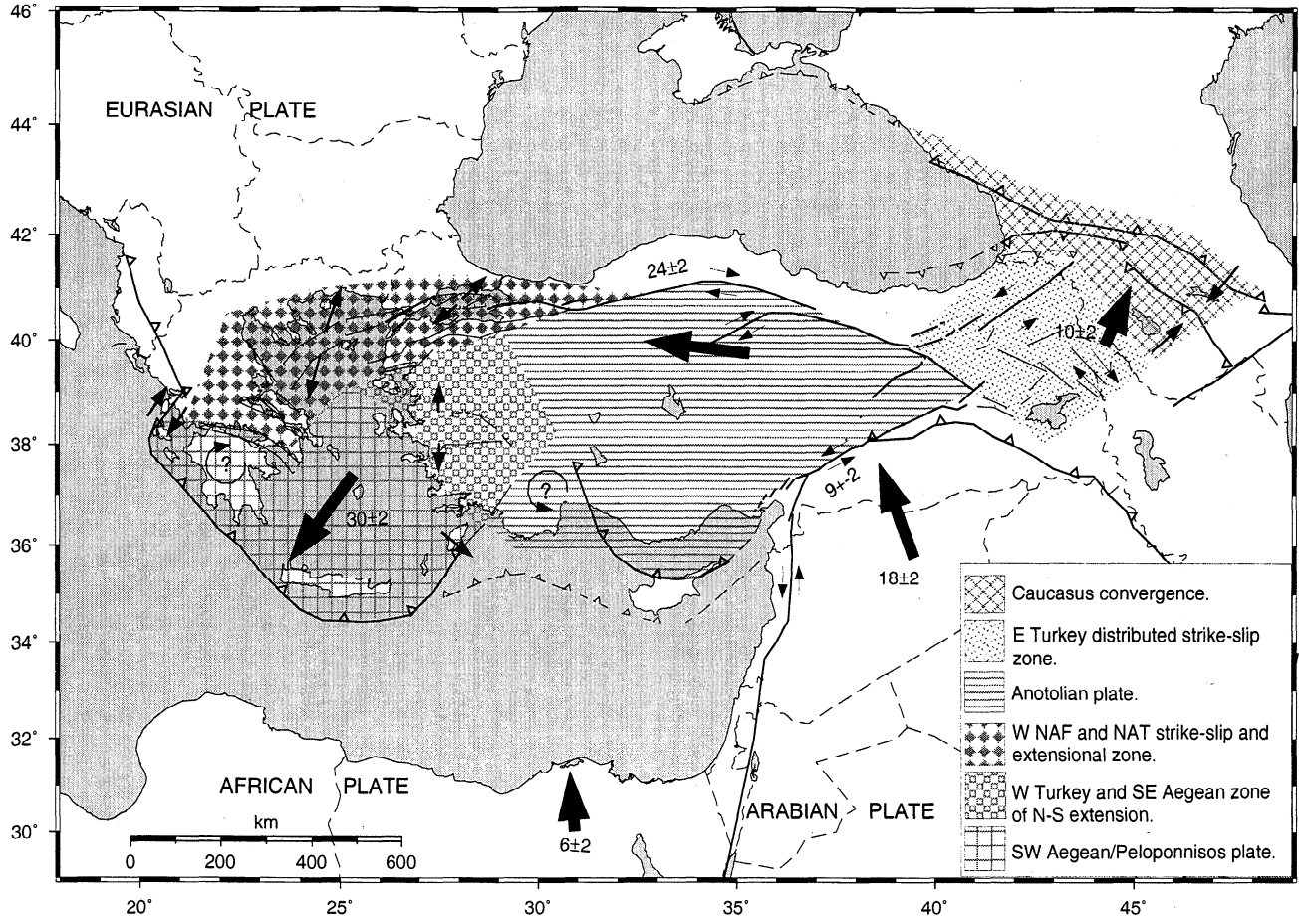

Figure 9. Schematic illustration of the principal results of this study. Hatching shows areas of coherent motion and zones of distributed deformation (see legend). Heavy arrows indicate generalized regional motions. Tectonic symbols are as in Plate 1. NAT, north Aegean trough.

deformations for the eastern Mediterranean plate collision zone. The primary kinematic results of this study are illustrated in schematic fashion in Figure 9. We determine preliminary velocities for the northern part of the Arabian plate and the northeastern part of the African plate. The GPS data quantify the partitioning of Arabian-Eurasian plate convergence between right-lateral strike-slip faulting on NW-SE striking faults in eastern Turkey and thrusting along the Caucasus thrust front. Total shortening across the Lesser and Greater Caucasus is 10 ± 2 mm/yr, with ~60% of this shortening occurring across the Greater Caucasus. Central Turkey (Anatolia) moves in a coherent fashion with internal deformation <2 mm/yr. The motion of Anatolia is bounded on the north by the right-lateral North Anatolian fault and on the southeast by the left-lateral East Anatolian fault. Upper bounds on fault slip rates for these faults are 24 ± 1 mm/yr and 9 ± 1 mm/yr, respectively. Relative to Eurasia, the southwestern Aegean-Peloponnisos moves toward the SSW at 30 ± 2 mm/yr in a coherent fashion with low internal deformation (<2 mm/yr). The southeastern Aegean region deviates significantly from this coherent motion, rotating counterclockwise and moving toward the Hellenic trench (i.e., toward the SE) at 10 ± 1 mm/yr relative to the southwestern Aegean. Right-lateral strike-slip deformation associated with the NAF extends into the north Aegean (north Aegean trough) terminating near the Gulf of Corinth. The north Aegean trough and Gulf of Corinth form the principal northern boundary of the southwestern Aegean plate. The southern Aegean is separated from Anatolia by a zone of N-S extension in western Turkey (Western Turkey Extensional Province). The overall kinematic pattern provided by GPS for Anatolia and the Aegean is qualitatively similar to that proposed by *McKenzie* [1970].

On the basis of this kinematic picture we speculate that the oceanic lithosphere of the Black and Caspian Seas form a resistant "backstop," diverting the impinging Anatolian plate to the west and "funneling" the continental lithosphere of eastern Turkey and the Caucasus around the eastern side of the Black Sea. We extend this hypothesis to explain the deviation of the western section of the NAF from the theoretical small

circle path (i.e., the fault deviates to the south to avoid the Black Sea lithosphere). This deviation may also account, in part, for the opening of the Sea of Marmara.

The rapid motion of the southwestern Aegean plate requires that forces other than pushing from Anatolia contribute to this motion; presumably forces associated with the foundering Africa plate as it subducts along the Hellenic trench. We hypothesize that the anomalous trenchward motion in the SE Aegean represents a response to particularly rapid sinking of the downgoing plate below this section of the arc, possibly associated with complex bending/breaking of the subducted plate at the Hellenic-Cyprus arc junction.

Acknowledgments. We are grateful to the hundreds of individuals who contributed to the acquisition of the GPS data that form the basis for this study. We appreciate the field support provided by the University NAVSTAR Consortium (UNAVCO) (James Stowell, Bruce Stephens, Doug Roberts, James Normandeau, and David Mencin), by Walter Hoppe (BKG), and by Dale Chayes, Lamont-Doherty Earth Observatory (LDEO). We acknowledge the cooperation of Durham University (Gillian Foulger) in coordinating their 1989 survey in western Turkey with those reported here and providing selected data for our analysis. We thank Shimon Wdowinski and Yosef Melzer for providing GPS data from Israel. We obtained both IGS tracking data and global analyses (solution files) from the Scripps Orbit and Permanent Array Center. The maps in this paper were generated using the public domain Generic Mapping Tools (GMT) software [*Wessel and Smith,* 1995]. We are especially grateful to Tom Herring for his development of the GLOBK software and discussions on the analysis and to James Jackson for helpful discussions on tectonic implications of the velocity field. The paper benefited from reviews by Yehuda Bock, Eric Calais, and Shimon Wdowinski. We thank Liz Henderson for formatting the manuscript for publication. This research was supported in part by the Hellenic General Secretariat for Research and Technology; Bundesamt fur Kartographie und Geodasie; ETH grant 41-2647.5; NASA grants NAS 5-33018 and NAG 5-1082 and NSF grant EAR86-19156 to LDEO; and NSF grants EAR-8709461, EAR-9304554, and NSF-9724114 and NASA grants NAGW-1961 and NAG5-6145 to MIT.

References

Alptekin, O., J.L. Nabelek, and M.N. Toksöz, Source mechanism of the Bartin earthquake of September 3, 1968 in northwestern Turkey: Evidence for active thrust faulting at the southern Black Sea margin, *Tectonophysics, 122,* 73–88, 1986.

Ambraseys, N.N., Studies in historical seismicity and tectonics, in *Geodynamics of Today,* pp. 7–16, Roy. Soc. of London, London, 1975.

Ambraseys, N.N., Engineering seismology, *Earthquake Eng. Struct. Dyn., 17,* 1–105, 1988.

Ambraseys, N.N., and J. A. Jackson, Faulting associated with historical and recent earthquakes in the eastern Mediterranean region, *Geophys. J. Int., 133,* 390–406, 1998.

Angelier, J., N. Lyberis, X. LePichon, E. Barrier, and P. Huchon, The tectonic development of the Hellenic arc and the Sea of Crete, a synthesis, *Tectonophysics, 86,* 159–196, 1982.

Armijo, R., B. Meyer, G.C.P. King, A. Rigo, and D. Papanastassiou, Quaternary evolution of the Gulf of Corinth rift and its implications for the Late Cenozoic evolution of the Aegean, *Geophys. J. R. Astron. Soc., 126,* 11–53, 1996.

Armijo, R., B. Meyer, A. Hubert, and A. Barka, Propagation of the North Anatolian fault into the northern Aegean: Timing and kinematics, *Geology, 27,* 267-270, 1999.

Arpat, E., and F. Saroglu, The East Anatolian fault system: Thoughts on its development, *Bull. Min. Res. Explor. Inst. Turkey, 78,* 33–39, 1972.

Avanessian, A., and S. Balassanian, Fault map of the Caucasus and eastern Turkey, paper presented at Second International Conference on Earthquake Hazard and Seismic Risk Reduction, UNESCO, Yerevan, Armenia, 1998.

Avouac, J.-P., and P. Tapponier, Kinematic model of active deformation in central Asia, *Geophys. Res. Lett., 20,* 895–898, 1993.

Barka, A., The North Anatolian fault zone, *Ann. Tectonicae, suppl. 6,* 164–195, 1992.

Barka A., Neotectonics of the Marmara Sea region, in *Active Tectonics of Northwestern Anatolia—The MARMARA Poly-Project,* edited by C. Schindler and M. Pfister, pp. 55–87, ETH Zurich, Zurich, Switzerland, 1997.

Barka, A., and P. Hancock, Neotectonic deformation patterns in the convex-northwards arc of the North Anatolian fault zone, in *The Geological Evolution of the Eastern Mediterranean,* edited by J.E. Dixon and A.H.F. Robertson, pp. 763–774, Geol. Soc. of London, London, 1984.

Barka, A., and K. Kadinsky-Cade, Strike-slip fault geometry in Turkey and its influence on earthquake activity, *Tectonics, 7,* 663–684, 1988.

Barka, A., and R. Reilinger, Active tectonics of the eastern Mediterranean region: Deduced from GPS, neotectonic, and seismicity data, *Ann. Geofis., 40,* 587–610, 1997.

Beutler, G., P. Morgan, and R. Neilan, Geodynamics: Tracking satellites to monitor global change, *GPS World, 4,* 40–46, 1993.

Bock, Y., J. Behr, P. Fang, J. Dean, and R. Leigh, Scripps Orbit and Permanent Array Center (SOPAC) and Southern Californian Permanent GPS Geodetic Array (PGGA), in *The Global Positioning System for the Geosciences,* pp. 55–61, Nat. Acad. Press, Washington, D.C., 1997.

Boucher, C., Z. Altamimi, and P. Sillard, Results and analysis of the ITRF96, *IERS Tech. Note 24,* 166 pp., Cent. Bur. of IERS, Obs. de Paris, Paris, France, 1998.

Burtman, V.S., Kinematics of the Arabian syntaxis, *Geotectonics, 23,* 139–146, 1989.

Butler, R.W.H., S. Spencer, and H.M. Griffiths, Transcurrent fault activity on the Dead Sea transform in Lebanon and its implications for plate tectonics and seismic hazard, *J. Geol. Soc. London, 154,* 757–760, 1997.

Chaimov, T.A., M. Barazangi, D. Al-Saad, T. Sawaf, and A. Gebran, Crustal shortening in the Palmyride fold belt, Syria, and implications for movement along the Dead Sea fault system, *Tectonics, 9,* 1369–1386, 1990.

Cisternas, A., and H. Philip, Seismotectonics of the Mediterranean region and the Caucasus, in *Historical and Prehistorical Earthquakes in the Caucasus,* edited by D. Giardini and S. Balassanian, *NATO ASI Ser. Environ., 28,* 39–77, 1997.

Clarke, P.J., et al., Crustal strain in central Greece from repeated GPS measurements in the interval 1989–1997, *Geophys. J. Int., 134,* 195–214, 1998.

Courtillot, V., R. Armijo, and P. Tapponier, The Sinai triple junction revisited, *Tectonophysics, 141,* 181–190, 1987.

Davies, R.R., P.C. England, B.E. Parsons, H. Billiris, D. Paradissis, and G. Veis, Geodetic strain in Greece in the interval 1892–1992, *J. Geophys. Res., 102,* 24,571–24,588, 1997.

De Jongc, M., M. Wortel, and W. Spakman, Regional scale tectonic evolution and the seismic velocity structure of the lithosphere and upper mantle, *J. Geophys. Res., 99,* 12,091–12,108, 1994.

DeMets, C., R.G. Gordon, D.F. Argus, and S. Stein, Current plate motions, *Geophys. J. Int., 101,* 425–478, 1990.

DeMets, C., R.G. Gordon, D.F. Argus, and S. Stein, Effects of recent revisions to the geomagnetic reversal time scale on estimates of current plate motions, *Geophys. Res. Lett., 21,* 2191–2194, 1994.

Dewey, J.F., M.R. Hempton, W.S.F. Kidd, F. Saroglu, and A.M.C. Sengor, Shortening of continental lithosphere: The neotectonics of eastern Anatolia—A young collision zone, in *Collision Tectonics,* edited by M.P. Coward and A.C. Ries, *Geol. Soc. Spec. Publ., 19,* , 3–36, 1986.

Dixon T., An introduction to the Global Positioning System and some geological applications, *Rev. Geophys., 29,* 249–276, 1991.

Dong, D., T.A. Herring, and R.W. King, Estimating regional deformation from a combination of space and terrestrial geodetic data, *J. Geod., 72,* 200–211, 1998.

Dotduyev, S.I., Nappe structure of the greater Caucasus Range, *Geotectonics, 20,* 420–430, 1986.

Dziewonski, A.M., T.-A. Chou, and J.H. Woodhouse, Determination of earthquake source parameters from waveform data for studies of global and regional seismicity, *J. Geophys. Res., 86,* 2825–2852, 1981.

Feigl, K.L., et al., Space geodetic measurement of crustal deformation in central and southern California, 1984–1992, *J. Geophys. Res., 98,* 21,677–21,712, 1993.

Gamkrelidze, P.O., and Gamkrelidze I.P., Tectonics of the southern slope of the greater Caucasus (within Georgia), 81 pp., Metsniyereba, Tbilisi, Georgia, 1977.

Gilbert, L.E., K. Kastens, K. Hurst, D. Paradissis, G. Veis, H. Billiris, W. Hoeppe, and W. Schlueter, Strain results and tectonics from the Aegean GPS experiment, *Eos Trans. AGU, 75(16),* Spring Meet. Suppl., 116, 1994.

Hager, B.H., R.W. King, and M.H. Murray, Measurement of crustal deformation using the Global Positioning System, *Annu. Rev. Earth Planet. Sci., 19,* 351–382, 1991.

Herring, T.A., GLOBK: Global Kalman filter VLBI and GPS analysis program version 4.1, Mass. Inst. of Technol., Cambridge, 1998.

Houseman, G.A., and P.C. England, Crustal thickening versus lateral expulsion in the Indian-Asian continental collision, *J. Geophys. Res., 98,* 12,233–12,249, 1993.

Isacks, B., J. Oliver, and L.R. Sykes, Seismology and the new global tectonics, *J. Geophys. Res., 73,* 5855-5899, 1968.

Jackson, J., Partitioning of strike-slip and convergent motion between Eurasia and Arabia in eastern Turkey, *J. Geophys. Res., 97,* 12,471–12,479, 1992.

Jackson, J., and D.P. McKenzie, Active tectonics of the Alpine-Himalayan Belt between western Turkey and Pakistan, *Geophys. J. R. Astron. Soc., 77,* 185–246, 1984.

Jackson, J., and D. McKenzie, The relationship between plate motions and seismic tremors, and the rates of active deformation in the Mediterranean and Middle East, *Geophys. J. R. Astron. Soc., 93,* 45–73, 1988.

Jackson, J.A., and N.N. Ambraseys, Convergence between Eurasia and Arabia in eastern Turkey and the Caucasus, in *Historical and Prehistorical Earthquakes in the Caucasus,* edited by D. Giardini and S. Balassanian, *NATO ASI Ser. Environ., 28,* 79–90, 1997.

Jestin F., P. Huchon, and J.M. Gaulier, The Somalia Plate and the East African rift system: Present-day kinematics, *Geophys. J. Int., 116,* 637–654, 1994.

Joffe, S., and Z. Garfunkel, Plate kinematics of the circum Red Sea—A re-evaluation, *Tectonophysics, 141,* 5–22, 1987.

Kahle, H.-G., M.V. Muller, A. Geiger, G. Danuser, S. Meuller, G. Veis, H. Billiris, and D. Paradissis, The strain field in NW Greece and the Ionian islands: Results inferred from GPS measurements, *Tectonophysics, 249,* 41–52, 1995.

Kahle, H.-G., M.V. Muller, and G. Veis, Trajectories of crustal deformation of western Greece from GPS observations 1989–1994, *Geophys. Res. Lett., 23,* 677–680, 1996.

Kahle, H.-G., C. Straub, R. Reilinger, S. McClusky, R. King, K. Hurst, G. Veis, K. Kastens, and P. Cross, The strain field in the eastern Mediterranean, estimated by repeated GPS measurements, *Tectonophysics, 294,* 237–252, 1998.

King, R.W., and Y. Bock, Documentation for the GAMIT analysis software, release 9.7, Mass. Inst. of Technol., Cambridge, 1998.

Langbein, J., and H. Johnson, Correlated errors in geodetic time series: Implications for time-dependent deformation, *J. Geophys. Res., 102,* 591–603, 1997.

Le Pichon, X., N. Chamot-Rooke, S. Lallemant, R. Noomen, and G. Veis, Geodetic determination of the kinematics of central Greece with respect to Europe: Implications for eastern Mediterranean tectonics, *J. Geophys. Res., 100,* 12,675–12,690, 1995.

Lyberis, N., T. Yurur, J. Chorowicz, E. Kasapoglu, and N. Gundogdu, The East Anatolian fault: An oblique collisional belt, *Tectonophysics, 204,* 1–15, 1992.

Makris, J., The crust and upper mantle of the Aegean region from deep seismic soundings, *Tectonophysics, 46,* 269–284, 1978.

Mao, A., C. Harrison, and T., Dixon, Noise in GPS coordinate time series, *J. Geophys. Res., 104,* 2797–2816, 1999.

McKenzie, D.P., Plate tectonics of the Mediterranean region, *Nature, 226,* 239–243, 1970.

McKenzie, D.P., Active tectonics of the Mediterranean region, *Geophys. J. R. Astron. Soc., 30,* 109–185, 1972.

Molnar, P., and P. Tapponier, Cenozoic tectonics of Asia: Effects of a continental collision, *Science, 189,* 419–426, 1975.

Muller, S., and H.-G. Kahle, Crust-mantle evolution, structures and dynamics of the Mediterranean-Alpine region, in *Contributions of Space Geodesy to Geodynamics: Crustal Dynamics, Geodyn. Ser.,* vol. 23, edited by D.E. Smith and D.L. Turcotte, pp. 249-298, AGU, Washington, D.C., 1993.

Noomen, R., T. Springer, B. Ambrosius, K. Herzberger, D. Kuijper, G. Mets, B. Overgauauw, and K. Wakker, Crustal deformations in the Mediterranean area computed from SLR and GPS observations, *J. Geodyn., 21,* 73–96, 1996.

Oral, B., Global Positioning System (GPS) measurements in Turkey (1988–1992): Kinematics of the Africa-Arabia-Eurasia Plate collision zone, Ph.D. thesis, 344 pp., Mass. Inst, of Technol., Cambridge, 1994.

Peter, Y., H.-G., Kahle, M. Cocard, G. Veis, S. Felekis, and D. Paradissis, Establishment of a permanent GPS network across the Kephalonia fault zone, Ionian Islands, Greece, *Tectonophysics, 294,* 253–260, 1998.

Philip, H., A. Cisternas, A. Gviskiani, and A. Gorshkov, The Caucasus: An actual example of the initial stages of continental collision, *Tectonophysics, 161,* 1–21, 1989.

Plag, H.-P., et al., Scientific objectives of current and future WEGENER activities, *Tectonophysics, 294,* 177–223, 1998.

Platzman, E.S., J.P. Platt, C. Tapirdamaz, M. Sanver, and C.C. Rundle, Why are there no clockwise rotations along the North Anatolian fault zone?, *J. Geophys. Res., 99,* 21,705–21,715, 1994.

Rebai, S., H. Philip, L. Dorbath, B. Borissof, H. Haessler, and A. Cisternas, Active tectonics in the Lesser Caucasus: Coexistence of compressive and extensional structures, *Tectonics, 12,* 1089–1114, 1993.

Reilinger, R., et al., Global Positioning System measurements of present-day crustal movements in the Arabia-Africa-Eurasia plate collision zone, *J. Geophys. Res., 102,* 9983–9999, 1997a.

Reilinger, R., et al., Preliminary estimates of plate convergence in the Caucasus collision zone from global positioning system measurements, *Geophys. Res. Lett., 24,* 1815–1818, 1997b.

Robbins, J.W., P.J. Dunn, M.H. Torrence, and D.E. Smith, Deformation in the eastern Mediterranean, in *Proceedings of the First Turkish International Symposium on Deformations,* vol. 2, pp. 738-745, Chamber of Surv. Eng., Ankara, Turkey, 1995.

Royden, L., The tectonic expression of slab pull at continental convergent boundaries, *Tectonics, 12,* 303–325, 1993.

Sengor, A.M.C., The North Anatolian transform fault: Its age, offset and tectonic significances, *J. Geol. Soc. London, 136,* 269–282, 1979.

Sengor, A.M.C., N. Gorur, and F. Saroglu, Strike-slip faulting and related basin formation in zones of tectonic escape: Turkey as a case study, in *Strike-Slip Faulting and Basin Formation,* edited by K.T. Biddle and N. Christie-Blick, *Spec. Publ. Soc. Econ. Paleontol. Mineral, 37,* 227–264, 1985.

Smith, D.E., R. Kolenkiewics, J.W. Robbins, P.J. Dunn, and M.H. Torrence, Horizontal crustal motion in the central and eastern Mediterranean inferred from satellite laser ranging measurements, *Geophys. Res. Lett., 21,* 1979–1982, 1994.

Sonder, L., and P. England, Effects of temperature dependent rheology on large-scale continental extension, *J. Geophys. Res., 94,* 7603–7619, 1989.

Spakman, W., Delay-time tomography of the upper mantle below central Europe, the Mediterranean, and Asia Minor, *Geophys. J. Int., 107,* 309–332, 1991.

Stein R.S., and A.A. Barka, Stress triggering of progressive earthquake failure on the North Anatolian Fault, Turkey, since 1939, *Eos Trans. AGU, 76(46),* Fall Meet. Suppl., F533, 1995.

Stiros, S.C., Heat flow and thermal structure of the Aegean Sea and the southern Balkans, in *Terrestrial Heat Flow and Lithosphere Structure,* vol. 5, edited by V. Cermak and L. Rybach, pp. 395–416, Springer-Verlag, New York, 1991.

Straub, C., and H.-G. Kahle, Global Positioning System (GPS) estimates of crustal deformation in the Marmara Sea region, northwest Anatolia, *Earth Planet. Sci. Lett., 121,* 495–502, 1994.

Straub, C., and H.-G. Kahle, Active crustal deformation in the Marmara Sea region, NW Anatolia, inferred from GPS measurements, *Geophys. Res. Lett., 22,* 2533–2536, 1995.

Straub, C, H.-G. Kahle, and C. Schindler, GPS and geologic estimates of the tectonic activity in the Marmara sea region, NW Anatolia, *J. Geophys. Res., 102,* 27587–27601, 1997.

Taymaz, T., H. Eyidogan, and J. Jackson, Source parameters of large earthquakes in the East Anatolian fault zone (Turkey), *Geophys. J. Int., 106,* 537–550, 1991.

Thatcher, W., Microplate versus continuum descriptions of active tectonic deformation, *J. Geophys. Res., 100,* 3885–3894, 1995.

Triep, E.G., G.A. Abers, A.L. Lerner-Lam, V. Mishatkin, N. Zakharchenko, and O. Starovoit, Active thrust front of the Greater Caucasus: The April 29, 1991 Racha earthquake sequence and its tectonic implications, *J. Geophys. Res., 100,* 4011–4034, 1995.

Voidomatis, P., S. Pavlides, and G. Papadopoulos, Active deformation and seismic potential in the Serbomacedonian zone, North Aegean, *Tectonophysics, 179,* 1–9, 1990.

Wessel, P., and W.H.F. Smith, New version of the generic mapping tools released, *Eos Trans. AGU, 76,* 329, 1995.

Westaway, R., Seismicity and tectonic deformation rate in Soviet Armenia: Implications for local earthquake hazard and evolution of adjacent regions, *Tectonics, 9,* 477–503, 1990.

Westaway, R., Present-day kinematics of the Middle East and eastern Mediterranean, *J. Geophys. Res., 99,* 12,071–12,090, 1994a.

Westaway, R., Evidence for dynamic coupling of surface processes with isostatic compensation in the lower crust during active extension of western Turkey, *J. Geophys. Res., 99,* 20,203–20,224, 1994b.

Wilson, P., Kinematics of the eastern Mediterranean region and the WEGENER-MEDLAS Project, *GeoJournal, 14,* 143–161, 1987.

Wortel, M.J.R., and W. Spakman, Structure and dynamics of subducted lithosphere in the Mediterranean region, *Proc. K. Ned. Akad. Wet. Nat. Sci.,, 95,* 325–347, 1992.

Zhang, J., Y. Bock, H. Johnson, P. Fang, S. Williams, J. Genrich, S. Wdowinski, and J. Behr, Southern California Permanent GPS Geodetic Array: Error analysis of daily position estimates and site velocities, *J. Geophys. Res., 102,* 18,035–18055, 1997.

Zonenshain, L.P., M.I. Kuzmin, and L.M. Natapov, *Geology of the USSR: A Plate Tectonic Synthesis, Geodyn. Ser.,* vol. 21, edited by B.M. Page, 242 pp., AGU, Washington, D.C., 1990.

S. Balassanian, National Survey for Seismic Protection, Yerevan, Armenia.

A. Barka, Eurasian Earth Sciences Institute, Istanbul Technical University, Istanbul 80626, Turkey.

C. Demir, O. Lenk, and I. Sanli, General Command of Mapping, Ankara, Turkey.

S. Ergintav, TUBITAK, Marmara Research Center, Gebze 41470, Turkey. (semih@yunus.mam.gov.tr.)

I. Georgiev and V. Kotzev, National Academy of Sciences, Geodesy Department, Sofia, Bulgaria.

O. Gurkan, Kandilli Observatory, Bogazici University, Istanbul, Turkey.

M. Hamburger, Department of Geological Sciences, Indiana University, 1005 East Tenth Street, Bloomington, IN 47405. (hamburg@geology.indiana.edu.)

K. Hurst, Jet Propulsion Laboratory, Mail Stop 238-600, 4800 Oak Grove Drive, Pasadena, CA 91350. (hurst@cobra.jpl.nasa.gov.)

H. Kahle and Y. Peter, Institut fur Geodasie und Photogrammetrie, ETII Honggerberg, IIPV G 52, CH-8093 Zurich, Switzerland. (kahle@p.igp.ethz.ch.)

K. Kastens, Lamont-Doherty Earth Observatory of Columbia University, Palisades, NY 10964. (kastens@ldeo.columbia.edu.)

G. Kekelidze and M. Nadariya, Department of Geodesy and Cartography of Georgia, Tbilisi, Georgia.

R. King, S. McClusky, R. Reilinger, and M. N. Toksöz, Department of Earth, Atmospheric, and Planetary Sciences, Massachusetts Institute of Technology, Building 54, Room 620, Cambridge, MA 02139. (rwk@chandler.mit.edu; simon@chandler.mit.edu; reilinge@erl.mit.edu; toksoz@mit.edu.)

S. Mahmoud and A. Tealeb, National Research Institute of Astronomy and Geophysics, Helwan, Egypt.

A. Mishin and M. Prilepin, Joint Institute of Physics of the Earth, Molodezhnaya 3, Moscow 117296, Russia.

A. Ouzounis, D. Paradissis, and G. Veis, Higher Geodesy Laboratory, National Technical University, Dept. of Surveying Engineering, Heroon Polytechniou 9, Zographos 15773, Athens, Greece.

H. Seeger, Bundesamt fur Kartographie und Geodasie, D-60598 Frankfurt, Germany.

(Received November 3, 1998; revised September 22, 1999; accepted September 30, 1999.)